Recombinant Virus-Like Particles Presenting Epitopes for Antibody Generation

Tim McCulloch

A thesis submitted for the degree of
Bachelor of Biomedical Science with Honours

Department of Microbiology and Immunology, University of Otago, Dunedin, New Zealand

November 2012

Abstract

Virus-like particles (VLP) have been shown to be effective vessels for drug or gene delivery, and vaccination. Much research has focused on the generation of VLP carrying heterologous tumour antigens to initiate cell-mediated immunity against tumours, where the VLP enhances the immunogenicity of the attached antigen. However, VLP can also be modified to incorporate an antigen on the surface to facilitate antibody generation. Purification tags or specific coupling sites could also be incorporated onto the surface of the particles, improving their functionality. This study aimed to utilise the immune stimulatory properties of VLP to generate antibodies against a heterologous model antigen, producing a scaffold for delivery and enhancement of antibody mediated subunit vaccines. More specifically, Human Norovirus (HuNV) and Rabbit hemorrhagic disease virus (RHDV) capsid proteins were engineered to express the YG1 epitope from human tumour necrosis factor-alpha (hTNF-α) at positions predicted to be displayed on the surface of the VLP.

Amino acids positions 368 of HuNV and 306 of RHDV capsid proteins were identified in the literature as confirmed sites of peptide insertion, with each locating to the exposed loops of the capsid protein P domain. Recombinant gene constructs expressing the YG1 peptide at these sites were produced by PCR. VLP were expressed in a baculovirus expression system and purified using differential centrifugation and cesium chloride gradient separation. Following expression, recombinant VLP assembly was confirmed by electron microscopy, and while the RHDV VLP was less stable than HuNV, they were both able to form particles. Rats immunised with these recombinant VLP generated IgA and IgG antibodies specific for both the native VLP carrier and the YG1 epitope.

Thus initial data indicates that HuNV and RHDV VLP can be genetically engineered to act as vaccine delivery systems, leading to enhanced peptide based subunit vaccines. The confirmed insertion sites could also be used to incorporate purification tags, specific coupling sites, or allow multi-epitope capability, where peptides can be included at both the N-terminus and on the surface of the same VLP.

Acknowledgements

First and foremost I would like to acknowledge and thank my supervisor, Professor Vernon Ward, for giving me the opportunity to complete my honours project in his lab. His encouragement, advice and patience have been a big part of this being a successful year.

Special thanks go to Vivienne Young, for her assistance with everything technical, and Dr Zabeen Lateef and Sarah Scullion, for their assistance which everything to do with immunology. These three have been my first port of call for all difficulties throughout the year, and have always made themselves available to be pestered.

A final thank you goes to the rest of lab 705 for their constant assistance, with a special mention for Farah Al Barwani, who was always there to help at night and during the weekend.

Table of Contents

List of Tables

List of Figures

Abbreviations

AcMNPV	*Autographa californica* nuclear polyhedrosis virus
APC	Antigen presenting cell
BCA	Bicinchoninic acid
BSA	Bovine serum albumin
CIES	Carrier induced epitopic suppression
CD	Cluster of differentiation
CMI	Cell mediated immunity
CsCl	Cesium chloride
CTL	Cytotoxic T lymphocyte
DC	Dendritic cell
DNA	Deoxyribonucleic acid
dNTP	Deoxyribonucleotide triphosphate
ELISA	Enzyme linked immunosorbent assay
ER	Endoplasmic reticulum
FBS	Fetal bovine serum
HBV	Hepatitis B virus
HPV	Human papillomavirus
HRP	Horseradish peroxidase
hTNF-α	Human tumour necrosis factor-alpha
HuNV	Human norovirus
IgA	Immunoglobulin A
IgG	Immunoglobulin G
kDa	Kilodalton
LB	Luria broth
MOI	Multiplicity of infection
MHC	Major histocompatibility complex

OVA	Ovalbumin
PBS	Phosphate buffered saline
PCR	Polymerase chain reaction
PTA	Phosphotungstic acid
RHDV	Rabbit haemorrhagic disease virus
RIPA	Radio-immunoprecipitation assay
rpm	Revolutions per minute
SDS	Sodium dodecyl sulfate
SDS-PAGE	Sodium dodecyl sulfate polyacrylamide gel electrophoresis
SFM	Serum free media
Sulfo-SMCC	Sulfosuccinimidyl-4-(N-maleimidomethyl)cyclohexane-1-carboxylate
T.E.M	Transmission electron microscopy

1. Introduction

1.1 Vaccination

Vaccine technology has advanced since its inception in the 19th century. Initially, most vaccines were based on live attenuated pathogens which were able to proliferate and initiate an immune response without causing disease. However these vaccines can be problematic in immunocompromised individuals, as in rare cases they can revert to the virulent form and cause disease (5, 24). To overcome this, vaccines were produced which contained either a killed organism or a subunit of the organism. These are able to generate protective immune responses, without the risk of vaccine induced disease. Some vaccines utilise conjugation, where poorly immunogenic antigens, such as polysaccharides or peptides, are attached to highly immunogenic proteins such as attenuated toxins (3). These methods are widely used in vaccines today. The goal of vaccination is to generate a strong immune memory, where a vaccine exposes the host to an antigen in a controlled manner so when the host encounters the antigen again the pathogen will be cleared more rapidly.

1.2 Immune response

Initiation of the adaptive immune system leads differentiation of naïve B and $CD8^+$ T cells into effector cells, which produces immune memory. These memory cells are inactive within the host until a subsequent exposure to the antigen, at which time they can produce faster and more specific responses than naïve immune cells. The type of immune response generated by an antigen depends in part on whether the antigen is endogenous of exogenous (Figure 1).

The first type of presentation is of endogenous or intracellular antigen (Figure 2), reviewed in Guermonprez *et al.* (2002) (23). Briefly, some foreign antigens can be found inside or on the surface of human cells, such as viral or tumour antigens. These endogenous antigens can be broken down by host proteasomes and transported to the endoplasmic reticulum (ER), where they bind major-histocompatibility complex class I molecules (MHC I). These MHC I-antigen complexes are transported to the cell membrane and presented on the surface of the cell. The MHC I-antigen complex is recognised by $CD8^+$ T lymphocytes, providing an initial signal for proliferation and differentiation into cytotoxic T lymphocytes (CTL). These cells act as effector cells, recognising the MHC I-antigen complex on other infected cells and initiating cell death

through cytotoxin release. Differentiation of $CD8^+$ T cells also produce memory T cells, which are activated on subsequent exposure to the antigen. Presentation via this pathway is preferential for vaccines against viruses and diseases such as cancer.

The second is presentation of exogenous antigens (Figure 2), reviewed in depth by Watts (63). These antigens are extracellular (e.g. bacteria, toxins) and are taken up by professional antigen presenting cells (APC) such as dendritic cells (DC) at the site of infection by a process known as phagocytosis. The antigen is taken up into a phagosome, which then fuses with a lysosome (lipid membrane bound vesicles containing degradation enzymes) to form a phagolysosome. The antigen is degraded in the vesicles and binds to MHC II molecules, which are transported to the surface of the APC. These MHC II antigen complexes provide the first signal for activation and differentiation of $CD4^+$ T lymphocytes. These activated $CD4^+$ cells have different functions, one of which is the activation of B cells, allowing them to differentiate into plasma cells that act as effector cells by producing antibodies specific to the foreign antigen. Like $CD8^+$ T cells, differentiation of B cells also produces memory cells. This type of presentation is required for vaccines against extracellular antigens, such as bacteria, or when trying to produce specific antibodies.

Some exogenous antigens can be taken up by APCs and presented on MHC I through the endogenous pathway instead of being presented on MHC II, by a phenomenon known as cross presentation (2). In terms of vaccination, cross presentation allows an antigen to be delivered exogenously yet still generate a CTL response, making it beneficial for vaccines against viruses or tumours. The intracellular mechanisms of cross-presentation are unclear, however there seems to be multiple pathways by which it can occur (28). One such mechanism is the “proteasome dependant” or “cytosolic” pathway. By this mechanism, antigens are taken up by the APC and translocated to the cytosol. From here they are degraded by proteasomes, transported to the ER and processed as intracellular antigens on MHC I. Studies showing that cross-presentation can still occur in the presence of proteasome inhibitors suggest that other proteasome independent pathways are present.

Recently virus-like particles have been getting attention for their potential as a type of subunit vaccine, both against the virus from which the particle was derived and against non-viral antigens that can be attached to the VLP.

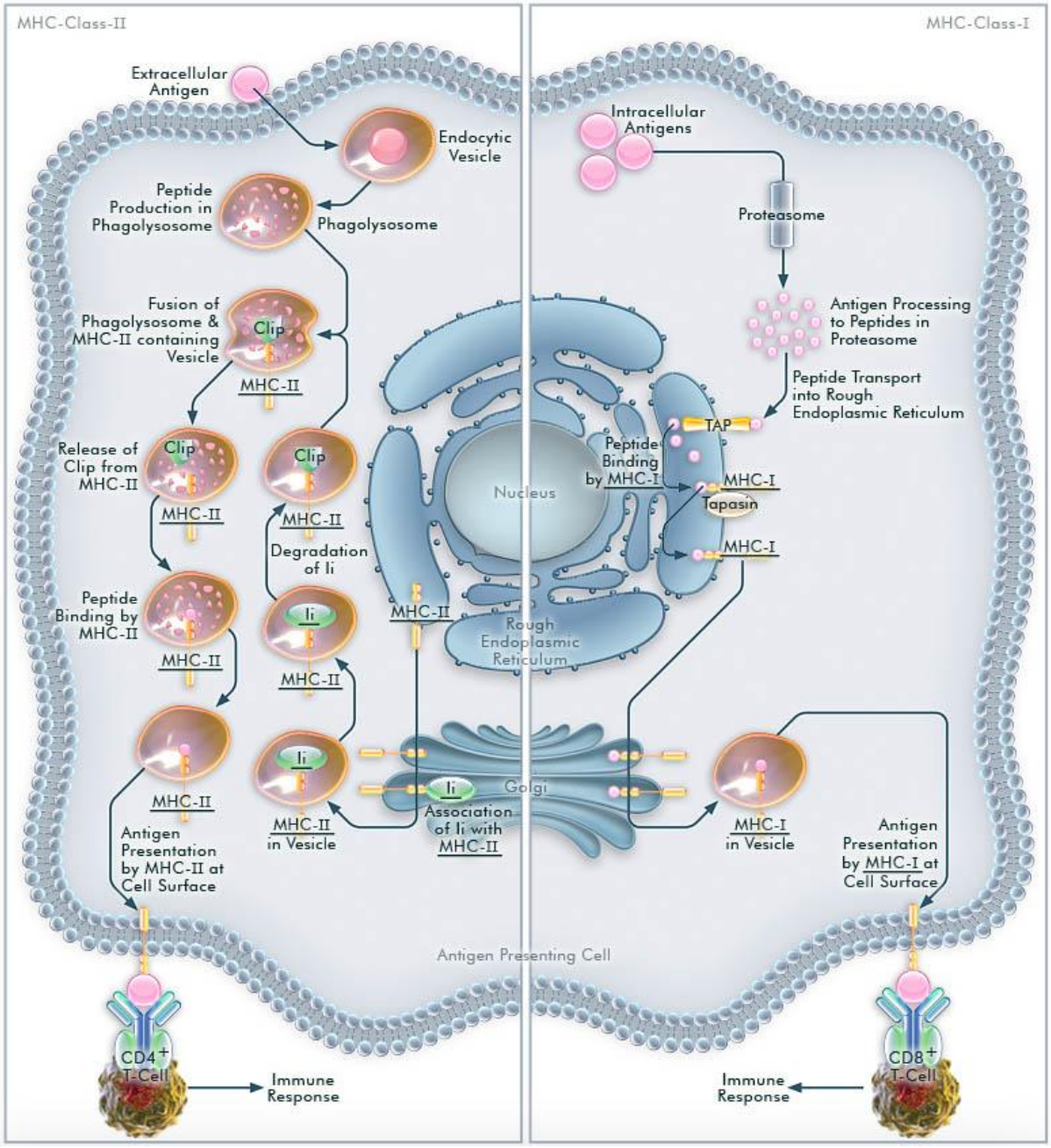

Figure 1. Major antigen presentation pathways[1]

Simplified diagram of the processing of extracellular or intracellular antigens by APCs to present them on MHC molecules. Extracellular antigen processing is shown on the left, where antigens are taken up by the APC, degraded in phagolysosomes and expressed on MHC-II. The MHC-II antigen complex is then presented to $CD4^+$ T cells. Intracellular antigen processing is depicted on the right, where endogenous antigens are degraded by proteasomes, transported to the ER and expressed on MHC-I. The MHC-I antigen complex is then presented to $CD8^+$ T cells.

[1] Figure adapted from eBioscience.com

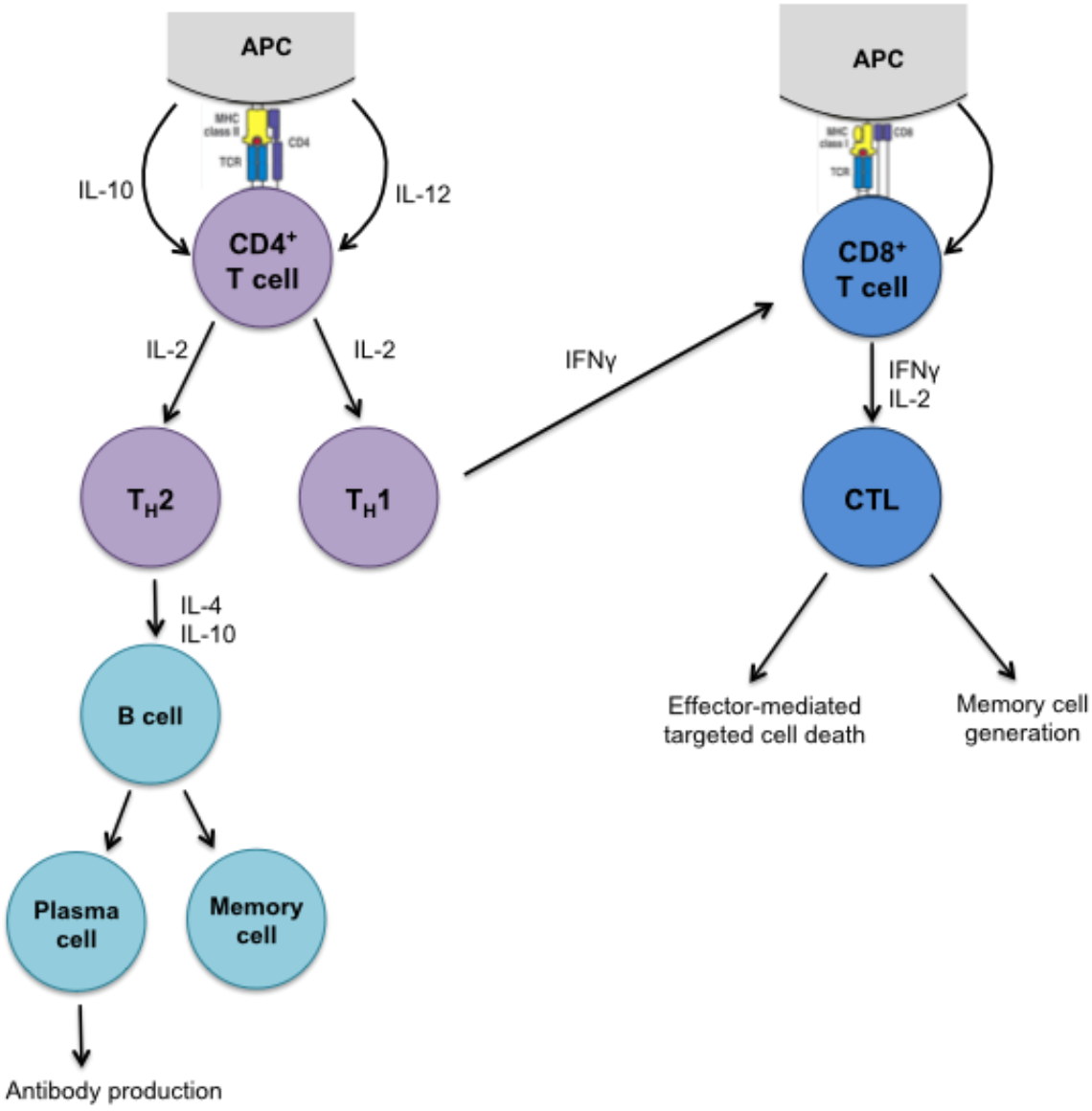

Figure 2. Presentation of exogenous or endogenous antigen leads to an immune response[2]

Simplified representation of immune response following presentation of exogenous or endogenous antigens, with the major cytokines shown. Exogenous antigen presentation is shown on the left, where $CD4^+$ T cells recognise MHC-II antigen complexes, leading to antibody production. Endogenous antigen presentation is shown on the right, where $CD8^+$ cells recognise MHC-I antigen complexes, stimulating their activation and differentiation into CTLs.

[2] Figure adapted from the Immune System Figure 3-19 (60)

1.3 Virus-like particles

Virus-like particles (VLP) are viral capsid shells that resemble their parent virus both morphologically and antigenically. They can be produced by expression of viral capsid genes in a recombinant expression system including *Escherichia coli* (7, 57), yeast (8, 66), plants (17, 51), and insect cells (27, 42). Their complex structure and high antigen copy number make them easily recognisable by the immune system and thus an ideal candidate for vaccination (34), stimulating both cellular and antibody immune responses (61, 62). VLP have the ability to traffic into draining lymph nodes, allowing them to be readily seen by antigen presenting cells (12). The size of VLP (20-150 nm) also increases immunogenicity as they appear to be near the optimal size for uptake into dendritic cells by endocytosis (18, 43). Because of their high immunogenicity, some studies have shown VLP to be effective as a vaccine in the absence of adjuvant (6, 35). They are however both non-replicating and non-infectious due the lack of genetic material, giving VLP based vaccines a safety advantage over live attenuated vaccines. VLP have been characterised for a range of viruses, including Rabbit hemorrhagic disease virus (RHDV) and Human Norovirus (HuNV) (Figure 3).

1.4 VLP as vaccines against parent virus

As VLP are antigenically identical to their parent virus, they provide protection against the parent virus and thus some are currently used as vaccines against these viruses. Human papillomavirus is a virus which infects the skin and mucosal membrane, leading to skin or genital warts, or cervical cancer. Live and attenuated vaccines against HPV are risky due to their inclusion of genetic material, which contains the E6 and E7 oncogenes (15, 52). Consequently, HPV VLP are used due to their high immunogenicity and no risk of vaccine-induced cancer (53). There are currently two available HPV vaccines: Cervarix and Gardasil. Both of these vaccines are protective against cervical cancer due to the inclusion of VLP derived from HPV 16 and HPV 18, which are the causative agents of 70% of cervical cancers. Gardasil also contains VLP from HPV 6 and HPV 11, which are the major causative agents of genital warts, allowing Gardasil to also provide protection against warts. Another example is Engerix-B, which is a vaccine against Hepatitis B virus (HBV) produced in yeast (40). This

vaccine is made up of hepatitis B surface antigen (HBsAg), which assembles into HBV VLP and provides protection against infection of the liver by Hepatitis B virus (4, 30).

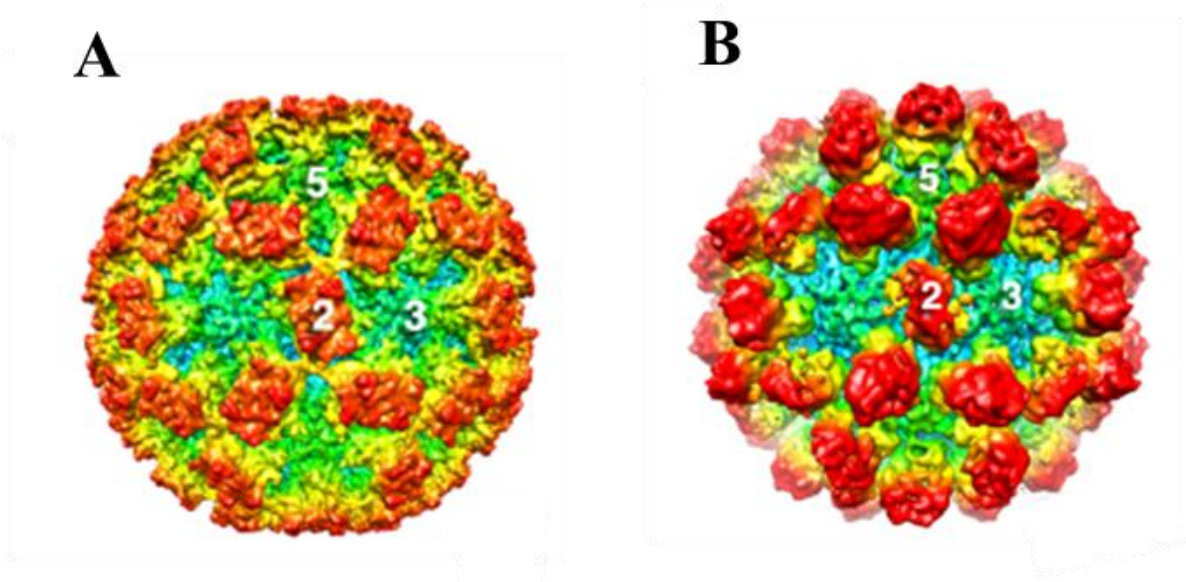

Figure 3. CryoEM representations of HuNV and RHDV VLP[3]

CryoEM diagrams of (**A**) HuNV VLP and (**B**) RHDV VLP, with radius colouring, shown at 1,500,000 times magnification. VLP show an icosahedral shape with 2, 3 and 5-fold axes of symmetry, as indicated by the numbers.

[3] Figure prepared by Katpally *et al* (2010)

1.5 VLP as vaccine delivery systems

Recent research has focused on using VLP as a vaccine delivery system, where antigens are attached to the particles. This is an interesting area of research as it may allow us to harness the strong immune stimulating properties of VLP to effectively vaccinate against non-viral, heterologous antigens. The VLP provides danger signals to the host, turning on immune pathways which recognise and initiate a stronger response against the heterologous antigen than if it was delivered alone. VLP are well characterised for the development of cell mediated immunity (CMI), due to their ability to be presented through the MHC I pathway via cross-presentation (65). This makes them a potential cancer vaccine candidate, an hypothesis which has been supported by the literature (65). Attachment of antigens to the VLP can be achieved by either chemical conjugation (46, 58) or genetic modification of native capsid proteins (31).

Chemical linkers can be used to conjugate proteins, peptides, nucleic acids, and other compounds to the surface of VLP (44), indicating the potential of conjugate VLP to be used for vaccine, drug or gene delivery (16, 21). Whilst conjugation has shown promise and given a proof of concept of antigen delivery using VLP, these methods can be problematic. The disadvantages of chemical conjugation include difficulty in quantifying the antigen, cost, loss of VLP and it is a time consuming process.

A more amenable method for wide spread use of VLP vaccines is to engineer the antigen into the capsid protein itself via genetic modification. By this method, every capsid protein produced will include the desired antigen. Traditionally for HuNV and RHDV VLP this has been done by insertion of the peptide at the N-terminus of the capsid protein, which locates the antigen on the inside of the VLP (36). This is effective for initiation of cell mediated immunity as the VLP are processed inside APCs and the epitope is seen as intracellular antigen. To stimulate a strong antibody response, the antigen must be displayed on the surface of the VLP so that it is seen as extracellular antigen. Producing recombinant VLP is likely more amenable to commercialisation as antigen can be quantified and there are no expensive or time consuming chemical conjugation steps after purification. However in some cases recombinant VLP may be subject to constraints such as the limited size of the antigen, poor VLP assembly and low particle yields.

1.6 Human Norovirus (HuNV)

HuNV is a member of the *Caliciviridae* family, which is responsible for 90% of nonbacterial gastroenteritis outbreaks in humans worldwide (33). The virus generally causes outbreaks in communities such as nursing homes, schools and cruise ships and is transmitted through the faecal oral route. The virus is highly infectious, with an infectious dose reported to be less than 20 virus particles (22). HuNV VLP can be produced by expression of the virus capsid protein VP58 in a recombinant expression system, where 180 copies self-assemble into a 40 nm VLP. This high copy number allows the VLP to present a large number of antigen copies to the immune system, making it highly immunogenic.

1.7 Rabbit hemorrhagic disease virus (RHDV)

Like HuNV, RHDV is a highly infectious member of the *Caliciviridae* family of viruses. It causes a largely fatal disease in rabbits characterised by fever, anorexia, paralysis and coma leading to death (1). RHDV VLP can also be produced by expression of the virus capsid protein VP60 in a recombinant expression system, where 180 copies self-assemble into a 40 nm VLP (32). RHDV VLP has been used as a vaccine in rabbits, providing protection against rabbit hemorrhagic disease (32). The high antigen copy number and complex structure make the VLP highly immunogenic.

1.8 Capsid protein structure

The structure of calicivirus capsid proteins has been well characterised (29, 48, 50). The HuNV VP58 and RHDV VP60 capsid proteins are made up of two domains: the N-terminal shell (S) domain and the C-terminal protruding (P) domain. In the virus, the S domain forms a shell around the viral genetic material and forms the base of calicivirus VLP. A hinge region connects the S domain to the P domain, which is further divided into the stem region (P1) and globular head (P2). It is important to understand the structure of the VLP capsid protein when considering genetic modifications, as any sequence changes may affect protein folding or VLP assembly (67). When inserting foreign epitopes for vaccination purposes, the location of the antigen in the assembled VLP is crucial as this will determine how the antigen will be displayed to the immune system. The P domain has multiple surface loops, which have been predicted be easily

accessible to the immune system and tolerate peptide insertions without compromising protein folding.

1.9 HuNV as a vaccine delivery system

Peptides have been inserted onto the surface of HuNV VLP without interfering with expression or assembly. One review by Herbst-Kralovetz gives examples of positions in the amino acid sequence of VP58 that are amenable to peptide insertion (25). Although no immunogenicity data was obtained, they confirmed that peptides of 9 or 15 amino acids in length could be inserted at amino acid positions 363, 378, and 427 without interrupting expression or assembly (specific peptides were not published).

Expression of the HuNV capsid protein protruding domain alone has been shown to produce a unique particle called a P particle (55, 56). Similarly to VLP formation, when this truncated protein is expressed in a recombinant system, 24 copies self-assemble into a P particle. Like HuNV VLP, these particles have been genetically modified to incorporate heterologous antigens for vaccination. In one study, rotavirus protein VP8 was engineered onto the surface of the P particle and when used as a vaccine was shown to significantly improve antibody titres against the antigen compared to VP8 delivered alone (54). This study is of particular interest due to the size of the antigen used. VP8 is 159 amino acids in length, which is much greater than any peptides that have been inserted onto the surface of VLP, suggesting that P particles can tolerate much larger inserts than VLP.

HuNV VLP carrying heterologous antigens have the potential to be used as a joint vaccine, against both native HuNV and the inserted antigen. However due to the limited amount of cross-protection between HuNV genogroups (22), a dual target vaccine using a single genogroup of HuNV VLP as the carrier may not provide significant protection against the virus in the real world.

1.10 RHDV as a vaccine delivery system

Research has suggested that calicivirus VLP are extremely versatile particles. Various research groups have used RHDV as a vaccine delivery system using both conjugation and chimeric VLP. Peacey *et al.* (2007) described a method by which the chicken ovalbumin (OVA) protein was conjugated to RHDV VLP using the hetero-bifunctional

chemical linker, sulfo-SMCC (45). This study showed that the immune stimulatory properties of the VLP were conferred to the OVA protein through delivery of the antigen to dendritic cells, enhancing the specific T cell response by 10-fold compared to OVA delivered alone. The size of the OVA protein is 385 amino acids, which is much larger than the size of peptide that can be genetically incorporated into VLP.

Recombinant RHDV VLP was produced by Nagesha *et al*. in 1999, who produced chimeric VP60 with a six amino acid epitope from bluetongue virus capsid protein VP7 (Btag). This study showed that RHDV VLP could tolerate inserts at both the N and C terminus of the capsid protein, however insertion at the C-terminus significantly reduced the antigenicity of the Btag epitope (41). This early data suggests that VLP modification was not as simple as N-terminal addition for internal display and C-terminus for surface display and a more in depth analysis of the capsid protein structure is needed to engineer epitopes onto the VLP surface.

Crisci *et al*. (2009) published results in which they developed chimeric RHDV VLP containing epitopes on the surface. They identified a surface loop of the P2 domain of RHDV VP60 and inserted a known $CD8^+$ T cell epitope of the OVA protein at this position (between amino acids 306 and 307) as well as at the N-terminus (10). Mice vaccinated against VLP with the epitope at the N-terminus were able to completely clear recombinant Vaccinia virus expressing OVA protein, while mice vaccinated against VLP with the epitope on the surface were comparatively ineffective at clearing the virus. As expected, the results from this study indicated that localisation of the epitope to the inside of the VLP is more conducive to initiation of cellular immunity. While this paper identified an insertion site for surface display of a peptide, the use of a $CD8^+$ T cell epitope meant that antibody production was irrelevant and thus not measured. A more recent paper by the same group showed a specific antibody response against a helper T cell epitope inserted at the N-terminus (11) and suggested that in an unpublished study they were able to generate a potent humoral immune response to a B cell epitope displayed on the surface of RHDV.

Whilst these preliminary results have given an indication of the potential for vaccines based on display of antigens on the surface of RHDV, there is no specific information on the generation of antibodies from surface engineered epitopes.

1.11 YG1 peptide

In terms of vaccine development studies, a model antigen is a peptide or protein that can be vaccinated against in animal models to test a potential vaccination system or method. While vaccination against many model antigens has no direct therapeutic function, they can be used in model animal systems to give a proof of concept of a hypothesised vaccine system, schedule, adjuvant or delivery route. The OVA protein, derived from chicken egg whites, is one of the most commonly used and best characterised model antigens (37, 39). For this study we will use an epitope of the cytokine human tumour necrosis factor alpha (hTNF-α) called YG1, identified by Dong *et al*. (2010) (14). While this study is only using YG1 as a model antigen, it has been suggested as a possible target for conditions where an overexpression of hTNF-α exacerbates disease, such as rheumatoid arthritis or Crohn's disease. Production of antibodies effective at blocking the cytokine at the YG1 epitope could provide an alternative to the current treatment, Infliximab (38). The 15 amino acid YG1 epitope is a B cell epitope and is thus ideal for the generation of antibodies and suitable for this study. The antibodies generated can also be tested in functional *in vitro* assays.

1.12 Aims

Whilst there is a lot of literature based on using VLP as a vaccine delivery system, genetic insertion of a model antigen onto the surface of RHDV and HuNV VLP for the generation of antibodies has so far gone unpublished. We propose that both VLP will tolerate insertion of the YG1 epitope at positions in VP58 and VP60 predicted to locate to the surface of each VLP. We also believe that the recombinant VLP with YG1 on the surface will produce an antibody response in rats to both the VLP carrier and the YG1 epitope.

The first aim of this project is to modify the VP58 and VP60 capsid proteins of HuNV and RHDV respectively to incorporate the YG1 epitope of hTNF-α at positions predicted to be displayed on the surface of assembled VLP.

The expression and purification of native RHDV and HuNV VLP are well characterised, however genetic modification of the capsid genes that make up these VLP may lead to reduced particle expression or assembly. Thus the second aim of this

project is to express the recombinant capsid genes using the baculovirus expression system and confirm VLP assembly by electron microscopy. Mass spectrometry will be used to confirm the inclusion of the YG1 epitope.

The third aim of this project is to test the ability of the chimeric VLP with YG1 on the surface to stimulate a humoral or antibody immune response in rats. Titres of IgA and IgG antibody specific for YG1, RHDV, and HuNV will be observed in the serum and lung of vaccinated rats.

Further study in to this area may help lead to development of a widely used VLP based vaccine system against heterologous antigens. This system could utilise a range of VLP and lead to both medical and agricultural vaccination.

2. Materials and Methods

2.1 Protein structure prediction

The structure of RHDV VP60 was predicted using iTASSER (University of Michigan, Ann Arbor, MI, USA) and viewed, along with the crystallised structure of HuNV VP58, in Protean 3D from the Lasergene suite of sequence analysis software (DNASTAR™ Inc, Version 3.1.1, Madison, WI, USA). Sites of potential surface peptide insertion were determined from the literature (10, 25), and identified on the 3D models. The YG1 epitope was included in the sequence of each capsid protein at the determined locations, and modified structures predicted by iTASSER.

2.2 Modification of Viral Capsid Genes

2.2.1 Primer design

Capsid protein constructs were produced for both VP58 and VP60 which contained the YG1 epitope at amino acid positions 368 and 306, respectively. Primers for the amplification of recombinant VP58 and VP60 capsid genes were designed using Lasergene suite of sequence analysis software (DNASTAR™). All primers used are in Table 1. To generate HuNV VP58 with YG1 inserted after amino acid 368 (HUNV-YG1.368), an internal forward and reverse primer including the YG1 peptide were designed and used with VP58 forward and reverse primers supplied by the lab. The two products were then combined in a third PCR reaction to amplify the full length gene, where they acted both as the template and primers due to the overlapping YG1 region (Figure 4). To generate RHDV VP60 with the YG1 peptide after amino acid 306 (RHDV-YG1.306), two internal primers were designed. The forward primer included the YG1 sequence along with a NheI restriction site and was used with a VP60 reverse primer, while the internal reverse primer included a NheI restriction site and was used with a VP60 forward primer. The NheI sites were included to ligate the two products together after digestion with NheI enzyme, producing the full length gene (Figure 5).

Table 1. Primers used to modify and sequence VP58 and VP60 capsid genes

Primer	Sequence (5' to 3')[1-3]
VP60F	GTGA**ATG**CCATGGAGGGCAAAGCCCG
VP60_NheIR	AGCTAGCACTGCCTTTTCTGTGGTC
YG1_306F	GGCAGTGCTAGCTACACT*AGATCATCTTCTCGAACCCCGAG TGACAAGCCTGTAGCCCAT*GGAAGCAACGCAAACA
VP60RC-term	CCCAATCCGATGAATTCAGACATA
VP60-YG1.C-TERM	GGAATTCA*ATGGGCTACAGGCTTGTCACTCGGGGTTCGAGA AGATGATCT*AGACCCGACATAAGAAAAGCCATTGG
HuNV.VLPF	AAGGATCCAAAA**ATG**AAGATGGCGTCGAATGACGC
HuNV.YG1R	T*ATGGGCTACAGGCTTGTCACTCGGGGTTCGAGAAGATGATC T*GGCAAATTGAACTCTACCCAG
HuNV.YG1F	C*AGATCATCTTCTCGAACCCCGAGTGACAAGCCTGTAGCCCA T*ACCGACACAGACAATGA
HuNV3aR	GGAATTC**TTA**TAATGCACGTCTACGC
VP58-YG1.C-TERM	GGAATTC**TTA***ATGGGCTACAGGCTTGTCACTCGGGGTTCGA GAAGATGATCT*AGACCCTAATGCACGTCTACGCCCCG
HuNV.VLPintF[4]	CCTGTGTTGATCCCCTTACCC
HuNV.VLPintR[4]	CCGACTGGAGTGAACTTTGTATTTT
VP60intF[4]	CTCGAACCTGTTACCAT
VP60intR[4]	CCAGTCACTACGGCATA

[1] Bold sequences indicate either start (ATG) or stop (TTA) codons

[2] Underlined sequences indicate restriction enzyme sites. NheI, GCTAGC; BglII, AGATCT; BamHI, GGATCC; EcoRI, GAATTC.

[3] Sequence in italics indicates the YG1 peptide

[4] Indicates primer used for sequencing

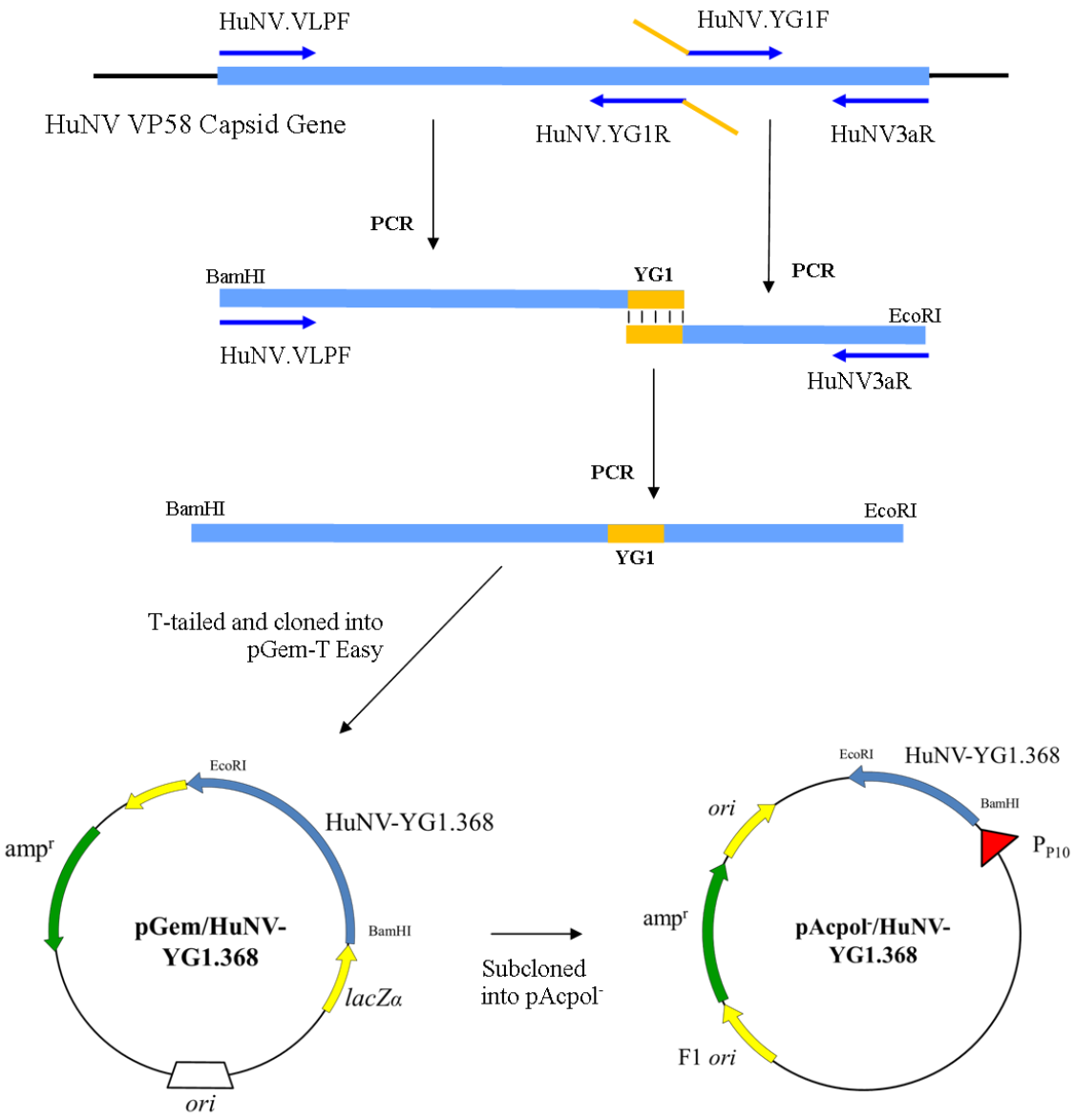

Figure 4. Schematic showing construction of HuNV-YG1.368 capsid gene

Primers were designed to amplify the VP58 gene and include the YG1 peptide at position 368. YG1 regions in the two initial PCR products overlap to combine the two products in the third reaction into the full length recombinant gene. The recombinant gene was cloned into pGem-T Easy for sequencing then subcloned into pAcpol$^-$ for co-transfection

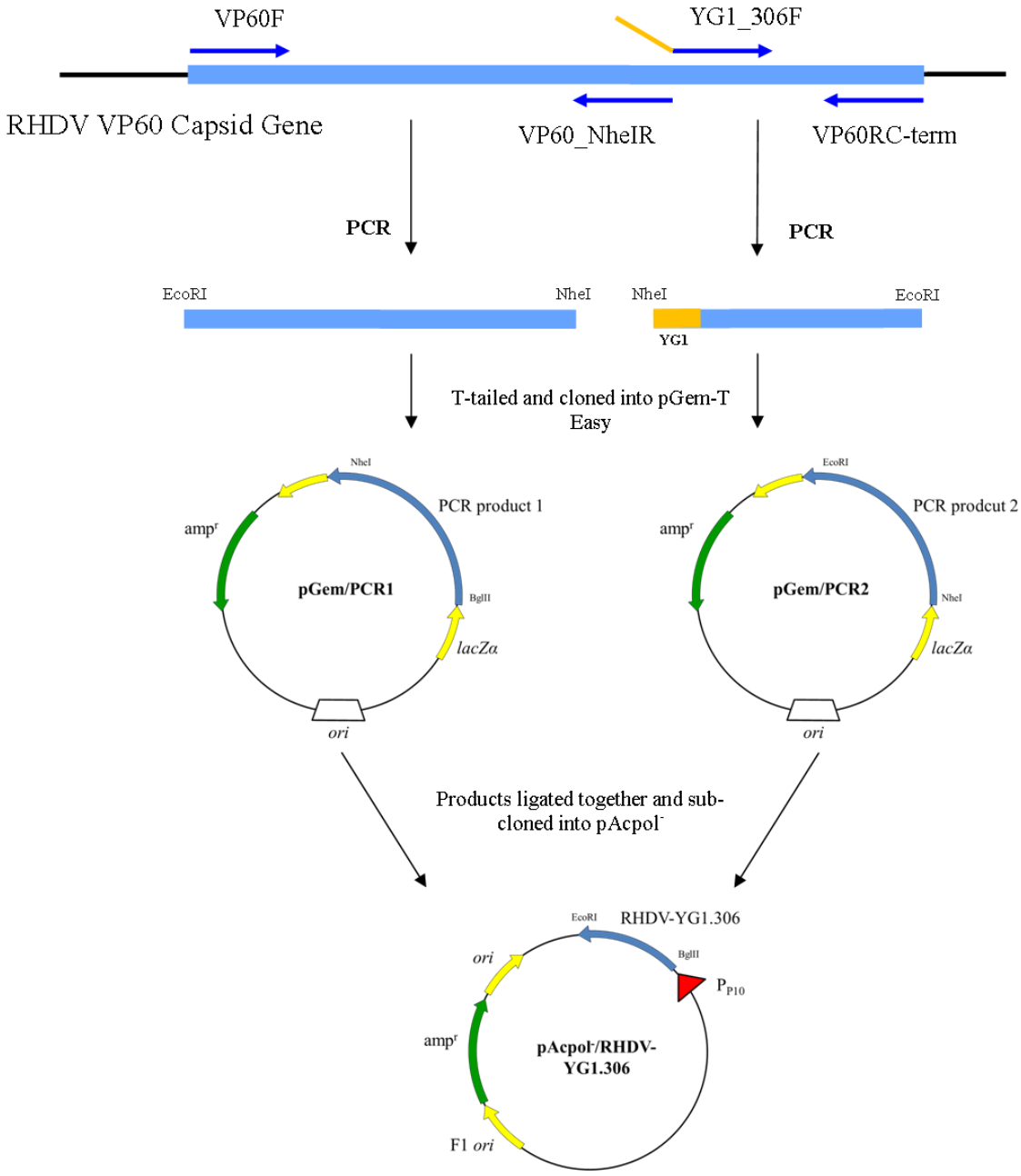

Figure 5. Schematic showing the construction of RHDV-YG1.306 capsid gene

Primers were designed to amplify the VP60 gene and include the YG1 peptide at position 306. The first PCR reaction amplified the N-terminal region of the gene and added a NheI restriction site at position 306. The second reaction amplified the C-terminal region of the gene and added the YG1 peptide and a NheI site at position 306. Each product was cloned into pGem-T Easy for sequencing. Each product was then subcloned into pAcpol$^-$ for co-transfection in a three way ligation, which generated the full length gene.

2.2.2 PCR protocols

All PCR reactions were performed using the Velocity PCR kit (Bioline Pty. Ltd, Australia). Reactions contained 10 µl of 5 x Buffer, 1 µl of DNA polymerase, 1 µl of 10 mM dNTP solution, 1 µl of each primer at 10 µM, 2-5 ng of VP60 or VP58 DNA template and made up to 50 µl with milliQ H_2O. The reaction to amplify full length HUNV-YG1.368 from the first products included 10 µl of 5 x Buffer, 1 µl of DNA polymerase, 1 µl of 10 mM dNTP solution, 7 ng of each PCR product, 1 µl of VP58 forward and reverse primers, and made up to 50 µl with milliQ H_2O. PCR cycles were performed in a Biometra TPersonal thermocycler (Biometra GmbH, Gottingen, Germany), as detailed in Table 2. PCR products were A-tailed immediately after the reaction using the tailing mix available in the Velocity PCR kit. The 50 µl PCR reaction was mixed with 5 µl of 10 x tailing mix and incubated at 37ºC for 5 minutes.

Table 2. Temperature cycles for the generation of PCR products

Cycle		**Temperature/Time**
Initial Denaturation		98°C, 2 min
Amplification[1]	Denaturation	98°C, 30 sec
	Annealing	50°C, 30 sec
	Elongation	72°C, 2 min
Final Elongation		72°C, 5 min

[1]Amplification was achieved through 30 cycles

2.2.3 Analysis of PCR products

PCR products were analysed by agarose gel electrophoresis using 1% Agarose LE (Roche Diagnostics GmbH, Mannheim, Germany) in 1 x TAE buffer (Appendix 1) in a Bio-Rad mini gel system (Bio-Rad, Hercules, CA, USA). Loading dye (3 µl, Appendix 1) was mixed with each sample before loading and the gel was run in 1 x TAE buffer at 100 volts for an hour. The gel was then stained in ethidium bromide solution (Appendix 1) for 30 minutes. DNA bands were visualised and photographed under ultraviolet (UV) light in a Bio-Rad ChemiDoc gel documentation system. Bands were excised

with a scalpel and DNA extracted using an AxyPrep DNA Gel Extraction kit (Axygen Biosciences, Union City, CA, USA).

2.2.4 Restriction digests

Restriction digests of PCR products, vectors and plasmids were all achieved in a 20 µl mixture. Each digest contained 1-5 µg of the DNA sample, 2 µl of the appropriate 10 x buffer (Roche), 10 units of the appropriate restriction enzymes and milliQ H_2O added to a total volume of 20 µl. HuNV-YG1.368 was digested with BamHI and EcoRI to produce sticky ends for ligation into a transfer vector digested with BglII and EcoRI. In order to ligate the two ends of RHDV-YG1.306 together to produce the full length gene and into the transfer vector, the N-terminal region was digested with BglII and NheI while the C-terminal region was digested with NheI and EcoRI. All digests were incubated at 37°C for 1-2 hours before analysis and extracted from a 1% agarose gel, as previously described.

2.2.5 Ligations

The gel purified restriction products of the recombinant VP58 and VP60 capsid genes were first ligated into pGem-T Easy (Promega, Madison, Wisconsin, USA) for sequencing, then subcloned into the transfer vector pAcpol$^-$ for co-transfection. Ligation mixes included 10-20 ng of insert DNA, 1 µl of T_4 DNA ligase, 2 µl of 10 x ligation buffer, 10 ng of pAcpol$^-$ vector (digested with BglII and EcoRI and gel purified), and made up to 20 µl with milliQ H_2O. As the RHDV-YG1.306 gene needed to be ligated together and into pAcpol$^-$, this mixture included 5 µl of each PCR product, 7 µl of pAcpol$^-$ DNA, 2 µl of 10 x ligation buffer and 1 µl of T_4 DNA ligase. All ligation reactions were mixed thoroughly and incubated overnight at 4ºC.

2.2.6 Transformation and screening

Ligation mixes or recombinant plasmids transformed into chemically competent *Escherichia coli* cells (strain XL1-Blue MRF). A 100 µl aliquot of calcium competent *E. coli* from -80°C stocks was thawed on ice for 30 minutes, before 10 µl of ligation mix or 2 µl of intact plasmid was added and incubated on ice for a further 30 minutes. The cells were then heat shocked at 37°C for 5 minutes before addition of 900 µl of pre-warmed LB broth (Appendix 1) and incubation for a further 60 minutes at 37°C.

The transformed cells (200 µl) were then spread onto LB agar (Appendix 1) containing ampicillin (50 µg/ml). When using pGem-T Easy, 50 µg/ml of X-gal (Progen Pharmaceuticals Limited, Darra, QLD, Australia) and 12 µg/ml of isopropyl-β-D-1-thiogalactopyranoside (IPTG) (Progen) were also added to allow for blue/white selection. The plates were left to stand for 5 minutes before inversion and overnight incubation at 37°C. Single white colonies were picked from the plates and used to inoculate separate 1.5 ml LB broths containing ampicillin (50 µg/ml). The cultures were grown at 37°C with shaking at 200 rpm for 14-16 hours before plasmids extracted using a AxyPrep Plasmid Miniprep Kit (Axygen Biosciences) and eluted in milliQ H_2O.

2.2.7 Sequencing of DNA

After amplification of successful transformations, the concentration of each plasmid sample was measured using a NanoDrop 1000 spectrophotometer (NanoDrop Technologies, Rockland, DA, USA). Sequences of recombinant capsid genes in the sequencing vector pGem-T Easy were checked by the Massey Genome Service (Massey University, Palmerston North, NZ). HuNV-YG1.368 sequencing samples were prepared in PCR tubes by dilution of DNA to 600 ng in a total volume of 28 µl milliQ H_2O. The universal M13 forward and reverse primers were used for the external primers, supplied by the Massey Genome Service. Due to the large size of the gene, external primers did not provide full coverage and thus internal primers were used. The internal primers were supplied by the lab (Table 1), and were added at a concentration of 6.4 pmol. RHDV-YG1.306 was sequenced as two separate segments before they were ligated together, consequently only the universal M13 forward and reverse primers were used. Sequence results were analysed using the SeqMan application from the Lasergene suite of the sequence analysis software (DNASTAR™).

2.3 Generation of recombinant baculoviruses

2.3.1 Co-transfection

Derivatives of *Autographa californica* nuclear polyhedrosis virus (AcMNPV) were used to produce recombinant baculoviruses expressing modified VLP using the BacVector 3000 expression system (Merck KGaA, Darmstadt, Germany). *Sf*21

(*Spodoptera frugiperda* IPLB-Sf21) insect cells were maintained in Sf900III serum-free medium (Invitrogen, Carlsbad, CA, USA). *Sf*21 insect cells were seeded onto 6 well plates at a concentration of 5 x 10^5 cells/ml, with 3 ml added to each well. Plates were incubated for 1 hour at 27°C to allow cells to adhere to the wells. The transfection mix was produced by adding 6 µl FuGene 6 (Roche) to 200 µl Sf900III SFM, which was added to a mix of 4 µl Bacvector 3000 DNA and ~1 µg of DNA encoding the modified capsid gene in the pAcpol$^-$ transfer vector. The mixture was incubated at room temperature for 30 minutes to allow the DNA to interact with the FuGene 6 liposomes. Medium was removed from the wells in the 6 well plate and the transfection mix was then added drop wise. Plates were incubated for 1 hour at room temperature, rocking every 20 minutes. To each well, 3 ml of Sf900III SFM was added with penicillin (0.2 U/ml) and streptomycin (0.2 µg/ml), and incubated for 3-5 days at 27°C. Medium containing recombinant virus was then removed from the experimental wells and stored at 4°C. Co-transfection was repeated for all both modified capsid genes so that separate stocks of baculovirus encoding HuNV-YG1.368 and RHDV-YG1.306 were produced.

2.3.2 Plaque assay

Recombinant baculoviruses were purified by plaque assay to separate them from wild type baculovirus. Six well plates were seeded with *Sf*21 insect cells at 5 x 10^5 cells/ml and incubated at 27°C for 1 hour. A tenfold dilution series of virus stocks from the co-transfections were set up in in Sf900III SFM to a concentration of 1 x 10^{-8}. One hundred microlitres of 1 x 10^{-3} to 10^{-8} dilutions were added to separate wells and incubated at room temperature for 1 hour, rocking every 20 minutes. Seven millilitres of molten 3% SeaPlaque agarose was mixed with 7 ml of Sf900III SFM containing 10% FBS (warmed to 41°C) and the mixture kept at 41°C. The medium was removed from each well, then wells were overlayed with 2 ml of the 50:50 agarose mixture and left to set at room temperature for 30 minutes. The overlay was then covered with 1.5 ml of Sf900III SFM containing 10% FBS, penicillin (0.2 U/ml) and streptomycin (0.2 µg/ml), and incubated at 27°C. After 4 days, 10 µl of 10% neutral red stain and 10 µl of X-gal were added to each well and incubated for 2 hours at room temperature. The media was removed and the plate was left at room temperature to allow the plaques to clear. Sterile Pasteur pipettes were used to pick clear (blue plaques indicate wild type virus), isolated plaques and used to inoculate separate 10 ml *Sf*21 cultures to propagate

the purified virus stock. Cultures were incubated at 27°C with shaking at 125 rpm for 4 days. After incubation, each culture was centrifuged for 5 minutes at 500 x g to pellet the cells. The supernatant containing the recombinant virus was decanted off, filter sterilised and stored at 4°C. Virus stocks were further amplified in 50 ml cultures and quantified by a plaque assay.

2.4 Production and purification of VLP

2.4.1 Expression of modified VLP

To express VLP, separate 400 ml *Sf*21 cultures were inoculated with the recombinant baculoviruses described earlier at a multiplicity of infection (MOI) of 1. Cultures were supplemented with penicillin (0.2 U/ml) and streptomycin (0.2 µg/ml). Infected cultures were incubated at 27°C for 3 days with shaking at 125 rpm and lids left loose to allow for aeration of cultures.

2.4.2 Purification of VLP

Modified VLP were harvested 3 days post infection. Samples from each culture were taken and cell viability checked by mixing 1:1 with trypan blue (Appendix 1) and checking on a haemocytometer. Cultures were treated with 0.5% Triton-X 100 (Sigma-Aldrich, St Louis, MO, USA) for 30 minutes to lyse cells and inactivate the recombinant baculovirus. Cellular debris was removed by centrifugation at 10,000 x g for 20 minutes in a F14 rotor (FIBERLite, Santa Clara, CA, USA). The supernatant was subjected to ultracentrifugation at 100,000 x g for 90 minutes in a Ti45 rotor (Beckman Coulter, Fullerton, CA, USA). The supernatant was discarded and the VLP pellets were resuspended in 1 ml of insect PBS (Appendix 1) at 4°C overnight. Tween-20 was added to each step at 0.01% for HuNV-YG1.368 samples.

To remove residual debris and aggregated material, resuspended VLP was centrifuged at 10,000 x g for 10 minutes. The supernatant was then loaded onto a cesium chloride (CsCl) gradient composed of 3 ml of 1.2 g/cm^3 CsCl underlayed with 3 ml of 1.4 g/cm^3 CsCl in SW32.1 polyallomer ultracentrifuge tubes. The tubes were centrifuged at 100,000 x g in a SW32.1 rotor (Beckman Coulter) for 18 hours. The VLP bands at the interface between 1.2 g/cm^3 and 1.4 g/cm^3 CsCl densities were harvested using a

Pasteur pipette and stored at 4°C. Tween-20 was added to each step at 0.01% for HuNV-YG1.368 samples.

2.4.3 Purification of RHDV-YG1.306

Due to the inability of RHDV-YG1.306 to form distinct VLP, an alternate purification method was developed. The protein was harvested from 400 ml cultures 3 days post infection. A sample was taken from the culture, mixed 1:1 with trypan blue and cell viability checked using a haemocytometer. Cultures were treated with 0.5% Triton-X 100 for 30 minutes to lyse cells. The insect cells were then pelleted by centrifugation at 10,000 x g for 20 minutes in a F250 rotor (Beckman Coulter). The pellets containing the insect cell debris were resuspended in a total volume of 20 ml of insect PBS and lysed using a Dounce homogenizer. Cells were then spun at 500 x g for 5 minutes to pellet the cellular material. Supernatant was taken and centrifuged again at 10,000 x g in a micro centrifuge. The pellets containing RHDV-YG1.306 were resuspended in a total volume of 4 ml insect PBS.

2.4.4 Sample dialysis

HuNV-YG1.368 and RHDV-YG1.306 in CsCl and iPBS respectively were dialysed extensively against coupling phosphate buffered saline (cPBS, Appendix 1) using 10,000 kDa molecular weight cut-off dialysis tubing. Tween-20 was added to the HuNV-YG1.368 sample at a concentration of 0.01% to prevent VLP aggregation. Buffer exchange involved a 2 hour, 4 hour, and overnight dialysis steps at 4°C. To concentrate the protein, the samples were then dialysed against 50% glycerol/cPBS for approximately 20 minutes or until the volume in the dialysis tubing decreased by half. Protein was then harvested from the dialysis tubing and extra glycerol added to a total concentration of 50%. Samples were stored at -20°C.

2.5 Analysis of VLP

2.5.1 SDS-PAGE (Sodium dodecyl sulfate-polyacrylamide gel electrophoresis)

VLP production and purity was confirmed by SDS-PAGE. Samples were diluted in milliQ H_2O to 0.2 mg/ml before being mixed 1:1 with 2 x sample buffer (Appendix 1)

and boiled for 5 minutes prior to loading. Samples were loaded onto a 10% SDS polyacrylamide gel (Appendix 1) along with Broad Range protein marker (NEB, Beverly, MA, USA) and electrophoresed in a Mini-PROTEAN III gel tank (Bio-Rad) in 1 x electrophoresis buffer (Appendix 1) at 180 V until the dye front reached the end of the gel. Gels were stained for 30 minutes with Coomassie Brilliant blue stain (Appendix 1) and soaked in destain solution (Appendix 1) with tissue paper to absorb excess stain until the protein bands were visualised.

2.5.2 BCA assay

Protein concentrations were analysed using a BCA (bicinchoninic acid) assay kit (Pierce, Rockford, IL, USA). A BSA protein standard at concentrations ranging from 25 µg/ml to 1500 µg/ml was made in RIPA buffer and added to separate wells in a 96 well plate in duplicate. VLP samples were diluted 1 in 10 in RIPA buffer and also added to separate wells in triplicate. To each well, 200 µl of reaction buffer was added (20:1 Reagent A:Reagent B) and incubated at 37°C in the dark for 30 minutes. The plate was then left in the dark at room temperature to cool down before being read using a Multiskan Ascent microplate reader at a wavelength of 595 nm and analysed using Ascent Version 2.4 software (Labsystems, Victoria, Australia). The data was transferred to GraphPad Prism v5.0 (GraphPad Software Inc., La Jolla, CA, USA), where the protein standards were used to produce a standard curve which allowed for the interpolation of sample protein concentrations.

2.5.3 Transmission electron microscopy (T.E.M)

VLP assembly was confirmed by viewing negatively stained VLP under the T.E.M. Samples were diluted to 0.2 mg/ml in milliQ H_2O then 10 µl was added to individual carbon coated grids and incubated for 1 minute. Excess sample was removed with filter paper. Grids were then negatively stained with 10 µl 1% phosphotungstic acid (PTA) at pH 6.8 which was immediately removed. The grids were then viewed using a Philips CM100 BioTWIN T.E.M (Phillips/FEI Corporation, Eindhove, Holland) and images captured using MegaVIEW III Soft Imaging System and iTEM Universal Imaging Platform (Soft Imaging System, Munster, Germany). Samples were prepared, stained and viewed at the Otago Centre for Electron Microscopy (University of Otago, Dunedin, New Zealand).

2.5.4 Mass spectrometry analysis

To confirm the presence of YG1 in the VLP, samples were run on an SDS-PAGE gel, the capsid protein band excised and submitted to the Centre for Protein Research (Department of Biochemistry, University of Otago, Dunedin, New Zealand). The excised protein samples were digested in the gel with trypsin then chymotrypsin before being analysed via an LTQ-Orbitrap hybrid mass spectrometer.

2.6 Vaccination

2.6.1 Animals

Specific pathogen free female Sprague Dawley rats (6-12 weeks old) were obtained from the Hercus Taieri Resource Unit, University of Otago, New Zealand. The University of Otago Animal Ethics Committee approved all experimental rat protocols under AEC permit 17/12.

2.6.2 Vaccination

Samples were diluted to 1 mg/ml in Dulbecco's phosphate buffered saline (dPBS, Appendix 1). Rats were subcutaneously injected with 200 µg of HuNV, HuNV-YG1.368, RHDV, RHDV-YG1.306 VLP or saline in 200 µl depending on vaccination group (Figure 6). HuNV and RHDV VLP used as vaccination negative controls were obtained from Dr Zabeen Lateef and Vivienne Young respectively. After 3 weeks, rats received a booster vaccination identical to their original vaccination. Three weeks after the booster vaccination, rats were euthanized by cervical dislocation and cardiac puncture under CO_2 for serum collection performed by Lesley Schofield. Lung lavage was also performed, assisted by Dr Zabeen Lateef and Sarah Scullion. Briefly, an incision was made above the larynx, muscles around the windpipe removed and windpipe cut three quarters through. A 14G catheter filled with 1 ml of PBS was inserted into the windpipe, lungs flushed out twice and PBS collected.

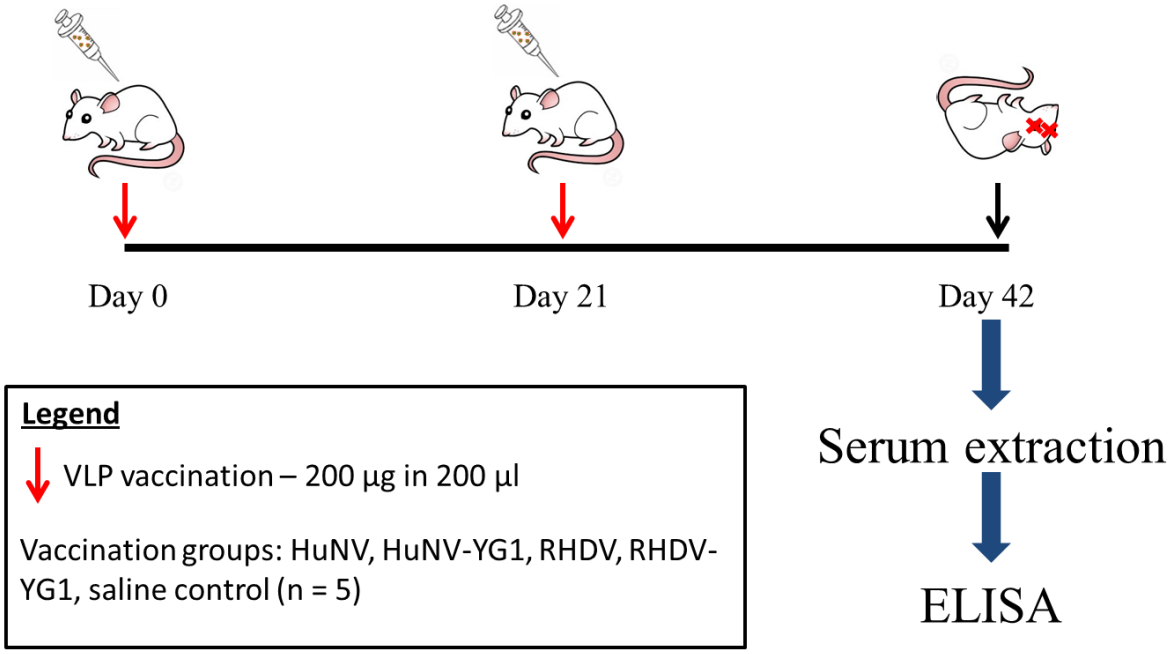

Figure 6. Vaccination schedule

Rats were vaccinated with 200 µg of VLP in 200 µl or a saline control, depending on vaccination group, at days 0 and 21. Each group contained 5 rats. At day 42, rats were euthanized by cervical dislocation under CO_2, serum extracted by cardiac puncture and lung lavage performed.

2.7 Antibody quantification

2.7.1 BSA coupling

YG1 peptide was coupled to Bovine serum albumin (BSA) to coat ELISA plates. BSA was dissolved in cPBS at a concentration of 5 mg/ml. Sulfo-SMCC (Thermo Fisher Scientific Inc., Rockford, IL, USA) was added at a 2 times molar excess and mixed for 30 minutes at room temperature. The mixture was dialysed extensively against cPBS for 2 then 4 hours, then overnight. BSA was harvested from the dialysis tubing and YG1 peptide with an extra cysteine residue (CRSSSRTPSDKPVAH) was added to a 10 x molar excess and mixed at room temperature for an hour to allow coupling to occur. Sulfo-SMCC is able to conjugate BSA to YG1 as the Sulfo-NHS ester group crosslinks with primary amine groups on the BSA, while the Sulfhydryl-reactive maleimide reacts with the cysteine residue on the YG1 peptide. The mixture was again dialysed against coupling PBS for 2 hours, 4 hours and overnight. YG1 coupling was confirmed by SDS-PAGE analysis and stored in aliquots at -80°C.

2.7.2 ELISA

The IgG antibody response in vaccinated rat serum was quantified with ELISA using a Rat IgG ELISA Quantitation Set (Bethyl Laboratories, Montgomery, TX, USA). Wells of 96 well plates were coated with 100 µl of either BSA-YG1 (2.5 µg/ml), HuNV VLP (10 µg/ml), or RHDV VLP (10 µg/ml) in cPBS and incubated for an hour at room temperature, or overnight at 4°C. Plates were washed 3 times in wash solution (Appendix 1). The wells were then blocked with 200 µl of blocking solution (Appendix 1) and incubated for an hour then washed 3 times. A 2 fold serial dilution of each rat serum sample in sample diluent (Appendix 1) to a total of 100 µl was added to separate wells, starting at a concentration of 1 in 100. A 1 in 2 serial dilution of an IgG standard (Bethyl Laboratories) was also included to wells initially coated with affinity purified anti-rat IgG antibody (Bethyl Laboratories). The plate was incubated for 60 minutes at room temperature or at 4°C overnight and washed 5 times. Antibody present was then detected by adding 100 µl of HRP detection antibody (Bethyl Laboratories) diluted to 1 in 20,000 in sample diluent. After incubating for an hour and washing 5 times, the signal was developed with 100 µl of TMB substrate (Boehringer, Mannheim, Germany) with incubation for a further 10-15 minutes in the dark at room temperature. The

reaction was stopped by adding 25 µl of 0.1 M HCl. Plate absorbance was read at 450 nm using a Multiskan Ascent microplate reader and Ascent Version 2.4 software. Data was transferred to Microsoft Excel and GraphPad Prism v5.0 for analysis. ELISAs were repeated to determine the IgA response in the serum to YG1, HuNV and RHDV using a Rat IgA ELISA Quantitation Set (Bethyl Laboratories), and also the IgG and IgA responses to YG1 in the lung lavage samples. Lung lavage sample dilutions started at 1 in 2 as opposed to 1 in 100 due to the expected low antibody titres.

2.7.3 Statistical analysis

Antibody titres were tested for statistical significance by performing unpaired two tailed student's *t*-tests using GraphPad Prism v5.0. Significance was assigned where the calculated *p*-value was 0.05 or less.

2.8 C-terminal modifications

Due to difficulties in RHDV-YG1.306 forming stable VLP, an alternate site of insertion was trialled. The YG1 peptide was inserted at the C-terminus of both HuNV VP58 and RHDV VP60 by PCR. The protocol used for PCR is shown in Table 2.

2.8.1 Primer design

Primers were designed for both VP58 and VP60 to include the YG1 peptide at the C-terminus (Table 1). To generate full length VP58 with the peptide at the C-terminus (HUNV-YG1.CTERM), a C-terminal reverse primer including the peptide was designed and used with a VP58 forward primer supplied by the lab (Figure 7A). To generate VP60 with the epitope at the C-terminus (RHDV-YG1.CTERM), a C-terminal reverse primer including the peptide was designed and used with a VP60 forward primer (Figure 7B). Primers were supplied by IDT (Coralville, Iowa, USA) and resuspended at a concentration of 100 µM in milliQ H_2O.

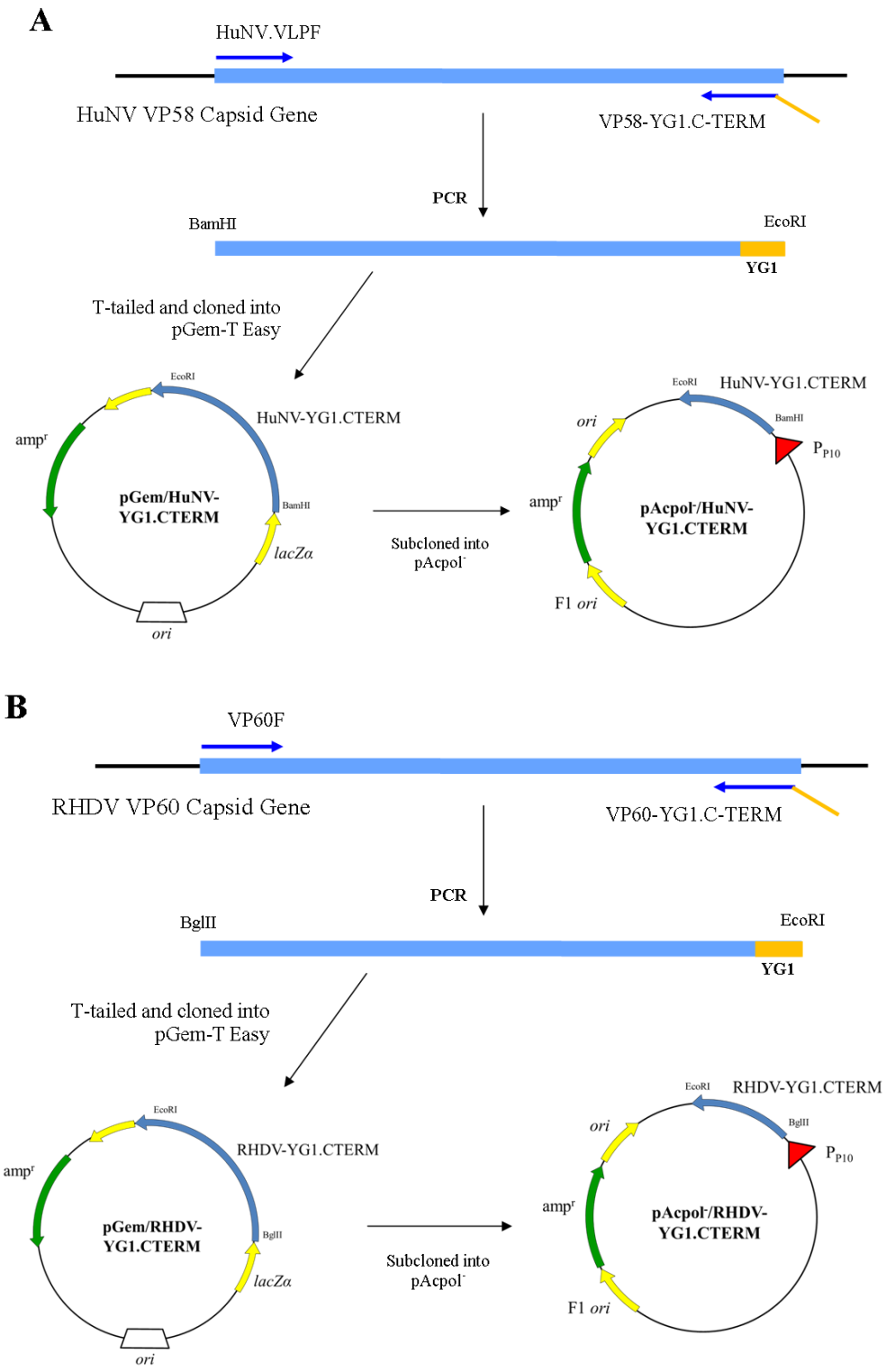

Figure 7. Schematic showing the construction of HuNV-YG1.CTERM and RHDV-YG1.CTERM capsid genes

Schematic showing the construction of **(A)** HuNV-YG1.CTERM and **(B)** RHDV-YG1.CTERM. Primers were designed to amplify the capsid genes and include the YG1 epitope at the C-terminus. Each product was cloned into pGem-T Easy for sequencing then subcloned into the transfer vector pAcpol$^-$

2.8.2 Construction of pAcpol$^-$ expressing VLP-YG1.CTERM

pAcpol$^-$ transfer vectors expressing HuNV-YG1.CTERM (Figure 7A) and RHDV-YG1.CERM (Figure 7B) were produced as previously described for the surface modified VLP (see section 2.2). Briefly, PCR products were A-tailed and gel purified from an agarose gel. Each gene was then ligated into pGem-T Easy for sequencing by the Massey Genome Service. The genes were sequenced using the universal M13 forward and reverse primers and internal forward and reverse primers supplied by the lab (Table 1). The genes were digested from the sequencing vector with restriction enzymes (BamHI and EcoRI for HuNV-YG1.CTERM, and BglII and EcoRI for RHDV-YG1.CTERM) and subcloned into the pAcpol$^-$ transfer vector. Each plasmid expressing the modified VLP was transformed into *E. coli* and prepped in 1.5 ml LB broths.

2.8.3 Generation of recombinant baculovirus

Recombinant baculovirus expressing HuNV-YG1.CTERM and RHDV-YG1.CTERM were produced by co-transfection and purified by plaque assay, as per the surface modified VLP (see section 2.3).

2.8.4 Production, purification and analysis of VLP

VLP were produced and purified by the similar methods as described for HuNV-YG1.368 (see section 2.4). Briefly, 50 ml insect cultures were infected with recombinant baculovirus and supplemented with penicillin and streptomycin. VLP were harvested 3 days post infection. Cells were lysed with 0.5% Triton-X 100 and subjected to differential centrifugation to separate the VLP from the cellular debris. VLP pellets were resuspended in a total of 2 ml iPBS and stored at 4°C. VLP were then diluted to 0.2 mg/ml in milliQ H_2O and visualised under a T.E.M.

3. Results

3.1 Capsid protein structure

The structure of HuNV VP58 and structure of RHDV VP60 predicted by iTASSER were viewed using Protean 3D (Figures 8 and 9). Points of confirmed epitope insertion were found in the literature, at amino acid position 368 for VP58 (25) and position 306 for VP60 (10). Based on the Protean 3D model, position 363 of VP58 and position 306 of VP60 were predicted to locate to the P2 region. With this in mind, amino acid 306 of VP60 was employed by this study to produce recombinant VLP, whilst VP58 employed amino acid 368 due to convenient nearby flanking GS residues. The structures of recombinant VP58 and VP60 incorporating the YG1 peptide at sites 368 and 306 respectively, were predicted by iTASSER and compared to the structures of the native VLP (Figure 8 and 9).

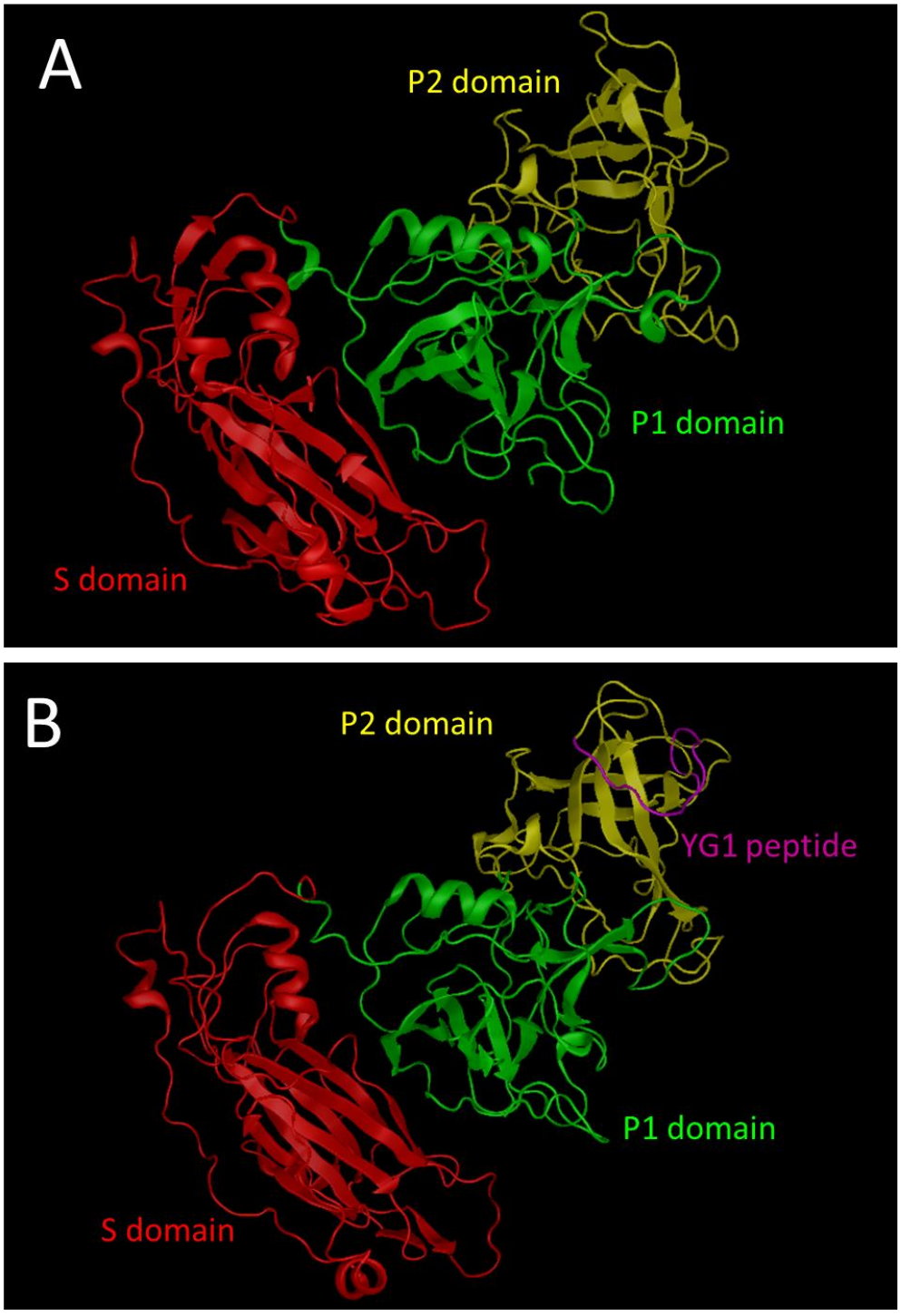

Figure 8. Structure of HuNV VP58

The known structure of HuNV VP58 **(A)** was compared to the structure of VP58 with YG1 inserted at position 368 **(B)**, predicted by iTASSER. The two domains (S and P) are shown. The purple section indicates the YG1 peptide at position 368, the intended site for peptide insertion.

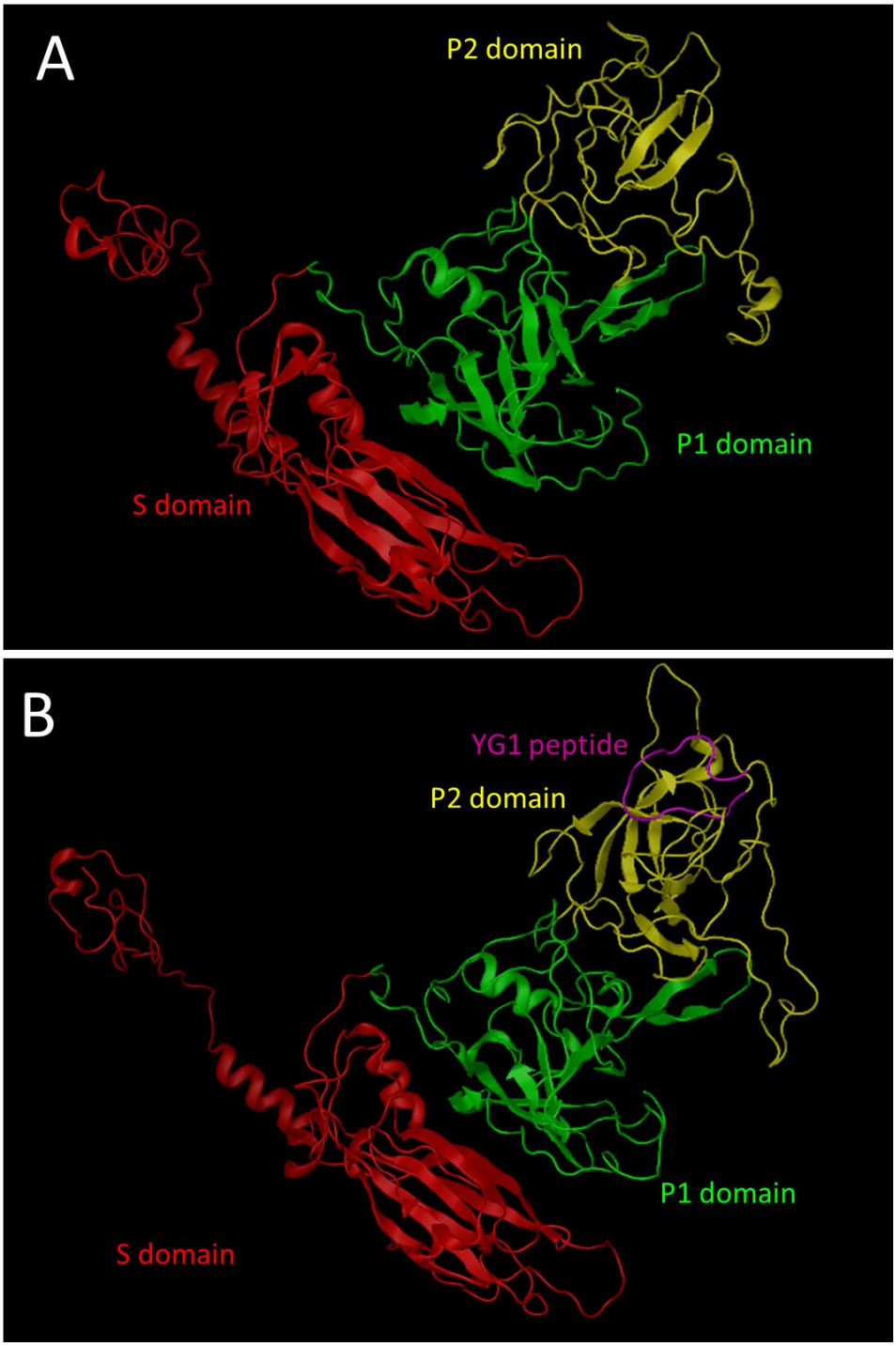

Figure 9. Predicted structure of RHDV VP60

Comparison of the structure of **(A):** RHDV VP60 capsid protein and **(B):** RHDV-YG1.306, predicted by iTASSER. The two domains (S and P) are shown. The purple section indicates the YG1 peptide at position 306, the intended site for peptide insertion.

3.2 Modification of viral capsid genes

The foreign amino acid sequence RSSSRTPSDKPVAH, encoding the YG1 epitope of hTNF-α, was engineered into HuNV VP58 and RHDV VP60 capsid genes by PCR at positions predicted to locate to the protruding (P) domain (Figure 10). Based on the literature, it was predicted that the amino acid positions 306 and 368 of RHDV VP60 and HuNV VP58, respectively, would be the most suitable for epitope insertion into the P domain. In each case, the hTNF-α derived sequence was flanked by glycine and serine (GS) residues, which may act as flexible linkers to promote assembly of the modified VLP. Insertion of the YG1 nucleotide sequence was confirmed by sequencing by the Massey Genome Service. Due to troubles with assembly of recombinant VP60, the C-terminus of each capsid protein was trialled as an alternative site of epitope insertion.

3.2.1 HuNV-YG1.368

PCR of pFastBac/VP58 using the primer pairs HuNV.VLPF/HuNV.YG1R and HuNV.YG1F/HuNV3aR produced products of sizes 1150 and 560 base pairs, respectively, confirmed by analysis on a 1% agarose gel (Figure 11A). These products were then combined in a third PCR reaction, where the overlapping YG1 sequence in each annealed to join the two sequences together, producing the full length gene of 1675 bp (Figure 11A). The gene was then ligated into pAcpol- to produce the plasmid pAcpol-/HuNV-YG1.368. Sequencing of the full length gene revealed a point mutation in the nucleotide sequence of HuNV-YG1.368. The nucleotide sequence showed an adenine instead of a guanine, which also changed the amino acid at position 340 from a nonpolar alanine to polar threonine.

3.2.2 RHDV-YG1.306

PCR of pAcpol-/VP60-SL using the primer pairs VP60F/VP60_NheIR and YG1_306F/VP60C-term produced products of sizes 915 and 900 bp, respectively, confirmed by analysis on a 1% agarose gel (Figure 11B). The Massey Genome Service confirmed the expected sequence of each, with the YG1 epitope included in the 900 bp sequence. The products were digested with restriction enzymes and ligated together and into a transfer vector (pAcpol) to produce pAcpol-/RHDV-YG1.306 (Figure 11B).

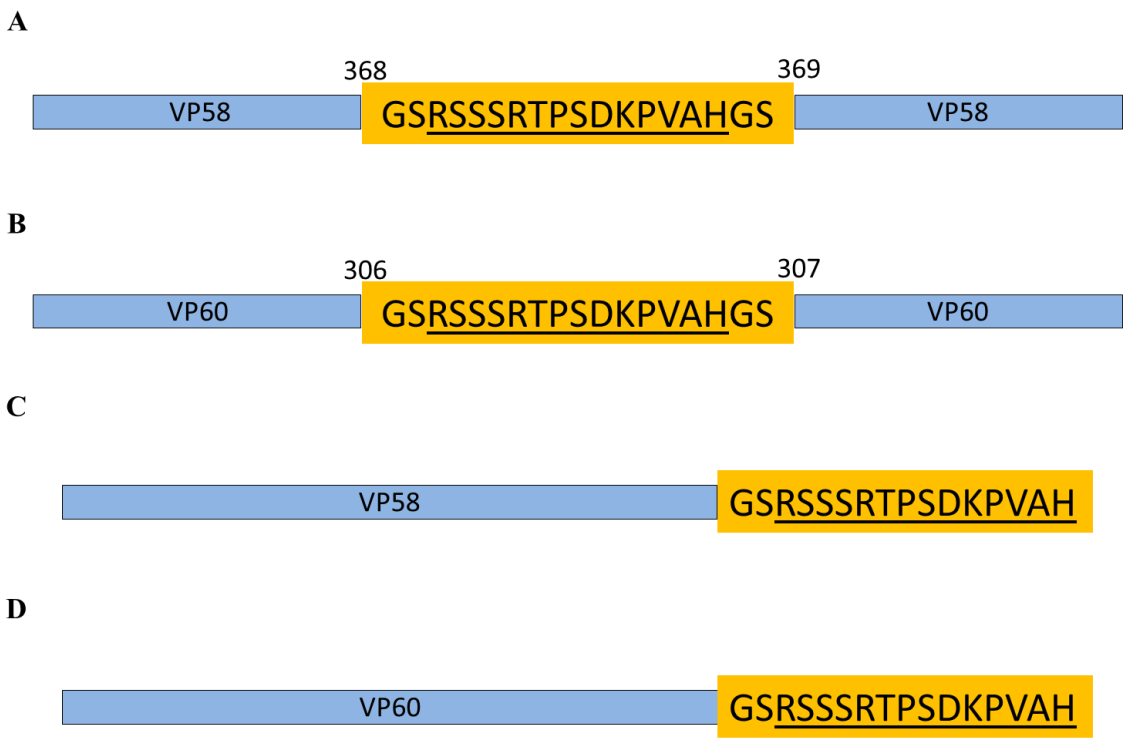

Figure 10. Recombinant VP58 and VP60 capsid gene constructs produced by PCR

The YG1 peptide sequence was inserted at different locations in the VP58 and VP60 capsid genes based on structural considerations. The sequence was inserted at position 368 of HuNV VP58 **(A)** and position 306 of RHDV VP60 **(B)** and the C-terminus of each gene **(C & D)**. YG1 sequence is underlined, flanked by GS linkers.

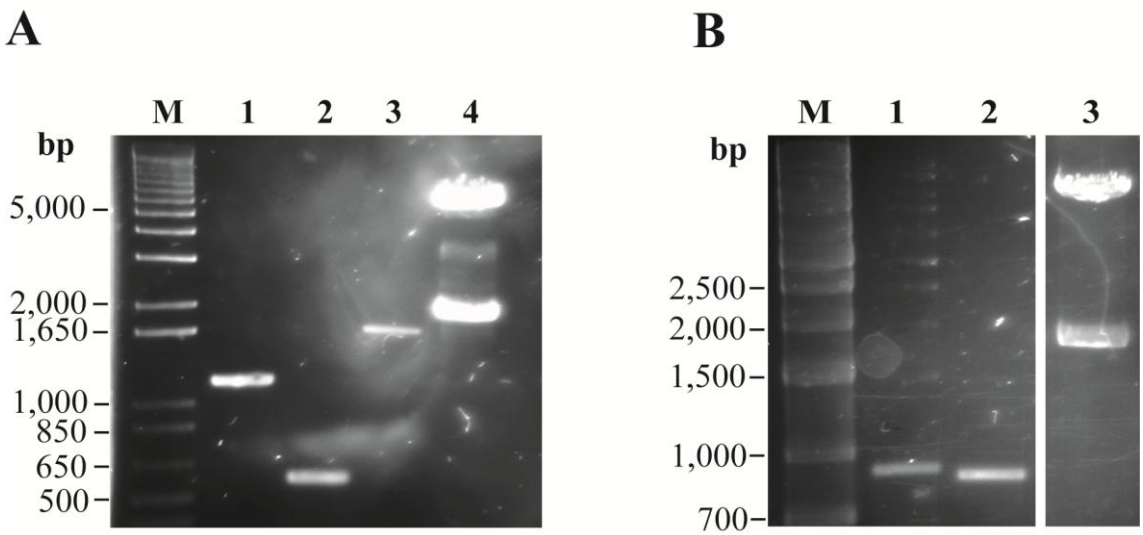

Figure 11. Modification of VP58 and VP60 capsid genes by PCR

A) Agarose gel showing the production of HUNV-YG1.368 by PCR; (1): PCR product one, 1150 bp, (2): PCR product two, 560 bp, (3): full length modified capsid gene produced by third PCR, 1675 bp, (4): full length gene in pAcpol- transfer vector, cut with BamHI and EcoRI, (M) 1kb plus ladder marker. **B)** Agarose gel showing production of RHDV-YG1.306 by PCR and ligation; (1): PCR product one, 915 bp, (2) PCR product two, 900 bp, (3) full length gene of 1815 bp produced by three way ligation into pAcpol- transfer vector, cut with BglII and EcoRI, (M) 1kb plus ladder marker.

3.3 Generation of recombinant baculovirus

Recombinant baculovirus expressing modified VLP were produced by co-transfection. Insect cells were transfected with the transfer vector containing the modified capsid protein and baculovirus DNA, allowing homologous recombination to occur between the two vectors to produce the recombinant baculovirus. Co-transfection was repeated to produce separate recombinant baculovirus expressing each of the four modified capsid genes. Each baculovirus was purified by plaque assay. X-gal present in the plaque assay turned wild type viral plaques blue. Consequently clear plaques (recombinant baculovirus) were picked and virus amplified in 50 ml insect cell cultures. A plaque assay was repeated on the amplified inoculums to determine viral titres, in order to infect cultures with an MOI of one. The estimated titre of recombinant HuNV-YG1.368 expressing baculovirus was 5.5×10^7 pfu/ml while titre of RHDV-YG1.306 expressing baculovirus was 4.8×10^7 pfu/ml.

3.4 Production and purification of VLP

VLP were expressed by infection of either 50 or 400 ml insect cell cultures with recombinant baculovirus. Following three-day incubation, cells were lysed and VLP were purified using differential centrifugation. Expression of the 58-60 kDa proteins was verified by analysing the purification fractions on a 10% SDS-PAGE gel (Figure 12). This analysis showed strong protein bands at the expected 58-60 kDa range in the 10,000 x g and 100,000 x g pellets of HuNV-YG1.368 purification. This is consistent with native HuNV VLP purification. In contrast, RHDV-YG1.306 was completely pelleted at 10,000 x g, where complete pelleting at 100,000 x g was expected. Consequently, an alternate purification protocol for this VLP was devised, as explained in Materials and Methods. HuNV-YG1.368 VLP was further purified based on its density on a CsCl gradient and both purified VLP samples were dialysed extensively against cPBS.

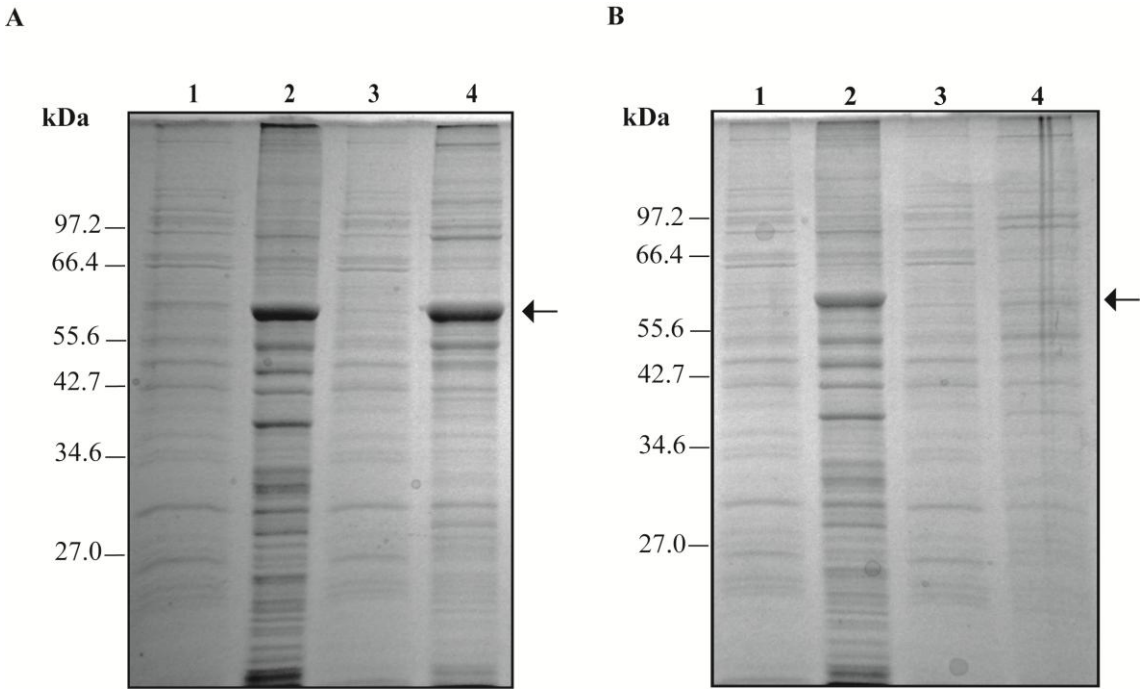

Figure 12. Production and purification of HuNV-YG1.368 and RHDV-YG1.306 VLP

A) SDS-PAGE gel showing fractions of differential centrifugation of HuNV-YG1.368 VLP. **B)** SDS-PAGE gel showing fractions of differential centrifugation of RHDV-YG1.306. Key: (1): 10,000 x g supernatant, (2): 10,000 x g pellet (resuspended), (3): 100,000 x g supernatant, (4): 100,000 x g pellet (resuspended). Positions of expressed proteins are indicated by arrows.

3.5 Analysis of VLP

To determine whether the recombinant capsid proteins assembled into VLP, purified samples were analysed using transmission electron microscopy. HuNV-YG1.368 was shown to spontaneously form VLP, visualised as characteristic 40 nm structures similar to native HuNV VLP (Figure 13A). Assembled VLP were not seen from initial 50 ml cultures infected with baculovirus expressing RHDV-YG1.306, however they were found in low numbers in infected 400 ml cultures (Figure 13B). Most of the protein in the recombinant RHDV samples formed protein aggregates (Figure 13C).

Analysis of concentration of purified VLP was made difficult due to inconsistencies between spectrophotometry with a Nanodrop 1000 and SDS-PAGE estimation. Consequently, BCA assay was performed on samples. Results from the BCA assay were taken into account and samples diluted to 0.2 mg/ml in sample buffer and analysed on SDS-PAGE (Figure 14) giving more consistent results. Estimated yields of protein from a 400 ml insect cell culture after dialysis ranged from 1-2 mg for HuNV-YG1.368 and 0.5-2 mg for RHDV-YG1.306.

When compared to their corresponding native VLP by SDS-PAGE, both of the surface modified versions showed a slight shift upwards, indicating an increase in size due to an inserted epitope (Figure 14). Orbitrap mass spectrophotometry was used to confirm the inserted epitope was the expected YG1 epitope. This technique confirmed that the YG1 epitope was present in the HuNV-YG1.368 sample, however it could not be found in the RHDV-YG1.306 sample.

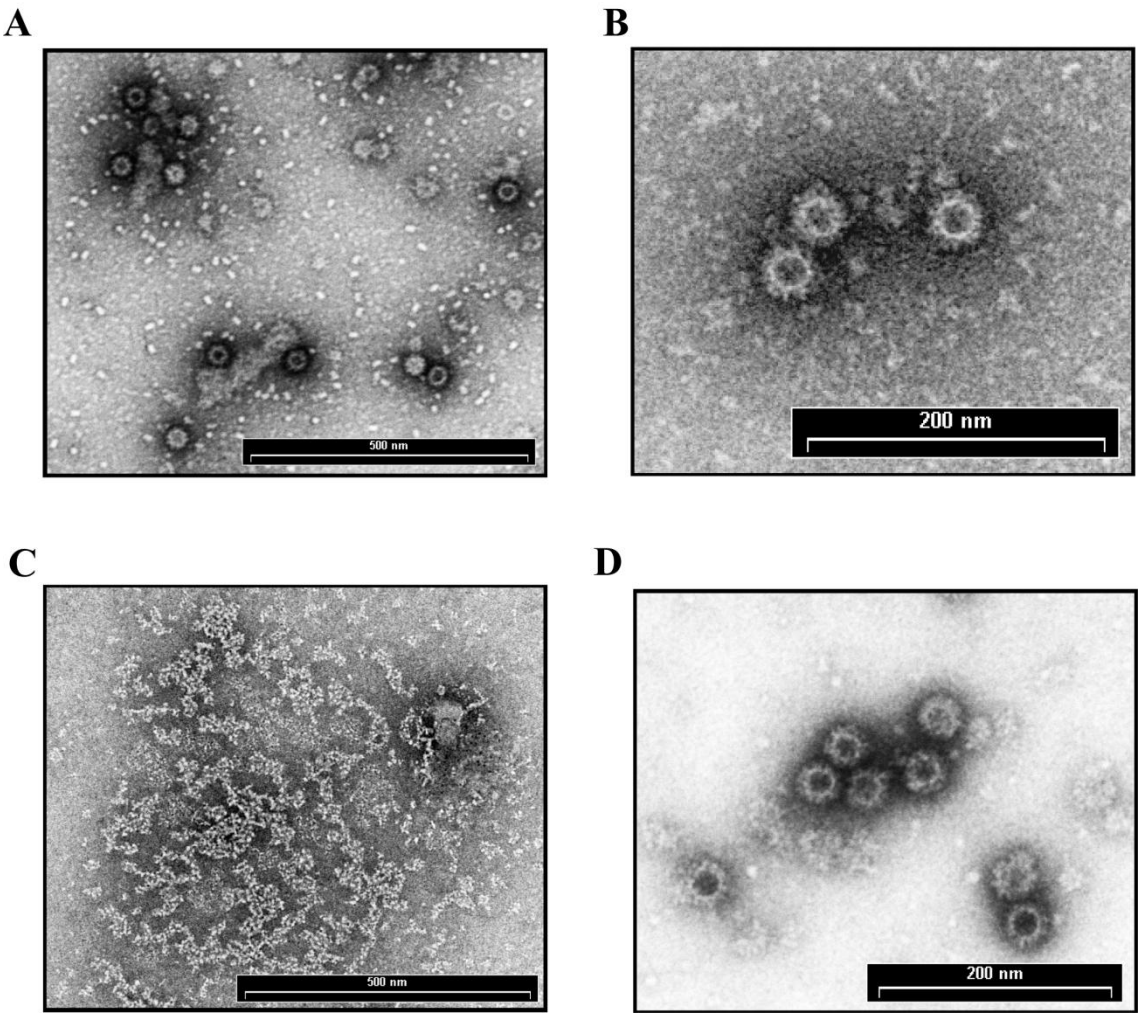

Figure 13. T.E.M of HuNV and RHDV derived VLP

VLP assembly was confirmed by viewing negatively stained samples under the T.E.M. **(A)**: HuNV-YG1.368 VLP, **(B)**: RHDV-YG1.306 VLP, **(C)**: RHDV-YG1.306 protein aggregates, **(D)**: RHDV-YG1.CTERM VLP. T.E.M showed that HuNV-YG1.368 and RHDV-YG1.CTERM assembled into stable VLP. RHDV-YG1.306 formed some VLP but most capsid protein was held as aggregates, and HuNV-YG1.CTERM did not form VLP at all (not shown).

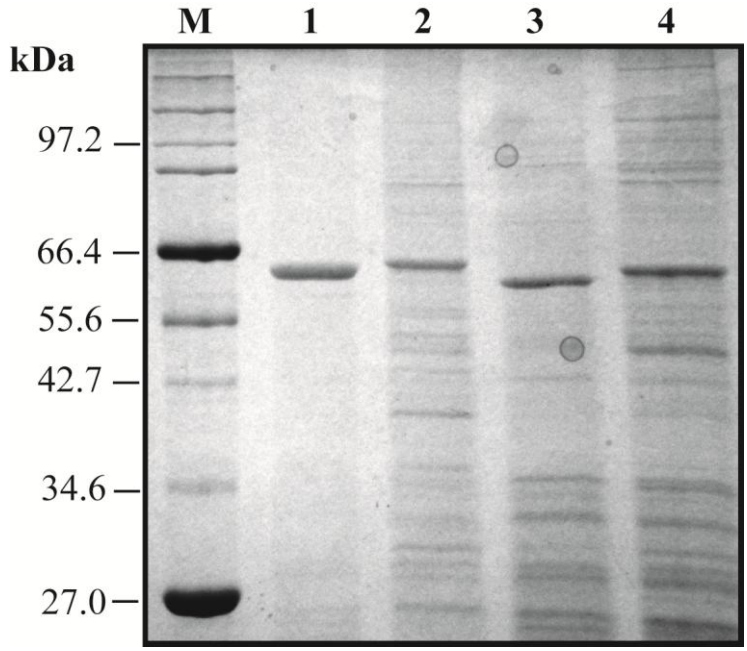

Figure 14. Modified capsid genes compared to native proteins

SDS-PAGE gel showing modified RHDV and HuNV capsid proteins compared to the capsid proteins from which they were derived (~58-60kDa). (1): RHDV control, (2): RHDV-YG1.306, (3): HuNV control, (4): HuNV-YG1.368, (M): Broad range protein marker. Samples were taken from vaccination preps and diluted to 0.2 mg/ml. Both recombinant VLP show a slight shift upwards on the gel compared to their parent VLP, indicating an increase in electrophoretic mobility due to an increase in size.

3.6 Antibody generation

In order to investigate the capability of the recombinant VLP to produce specific antibody responses against both the carrier and foreign epitope, female Sprague Dawley rats were subcutaneously vaccinated twice with HuNV, HuNV-YG1.368, RHDV or RHDV-YG1.306 VLP, or saline. Three weeks following the second vaccine, rats were euthanized under CO_2, serum extracted by cardiac puncture and lung lavage performed. ELISA was used to analyse levels of HuNV, RHDV, and YG1 specific IgG and IgA in the vaccinated rat serum, along with IgG and IgA specific for YG1 in the lung samples. Plates were coated with either HuNV or RHDV VLP, or BSA-YG1 depending on the specific antibodies investigating.

3.6.1 IgG in serum

All rats vaccinated with HuNV or HuNV-YG1.368 VLP elicited IgG antibody responses to native HuNV VLP (Figure 15A), with average titres of 702 µg/ml for HuNV VLP challenged rats and 268 µg/ml for those challenged with HuNV-YG1.368 (Figure 15B). Likewise, all rats vaccinated with RHDV or RHDV-YG1.306 VLP elicited IgG antibody responses to RHDV VLP (Figure 15C), with an average titre of 1398 µg/ml for rats vaccinated with RHDV and 1076 µg/ml for rats vaccinated with RHDV-YG1.306 (Figure 15D). Four out of the five rats vaccinated with HuNV-YG1.368 generated serum IgG responses to the YG1 epitope (Figure 16A), with an average titre of 15 µg/ml (Figure 16B), while all five rats challenged with RHDV-YG1.306 VLP generated antibodies against the YG1 peptide (Figure 16A), with an average titre of 32 µg/ml (Figure 16B). This gives confirmation that the YG1 peptide was present in both samples, despite not being found in RHDV-YG1.306 by mass spectrometry.

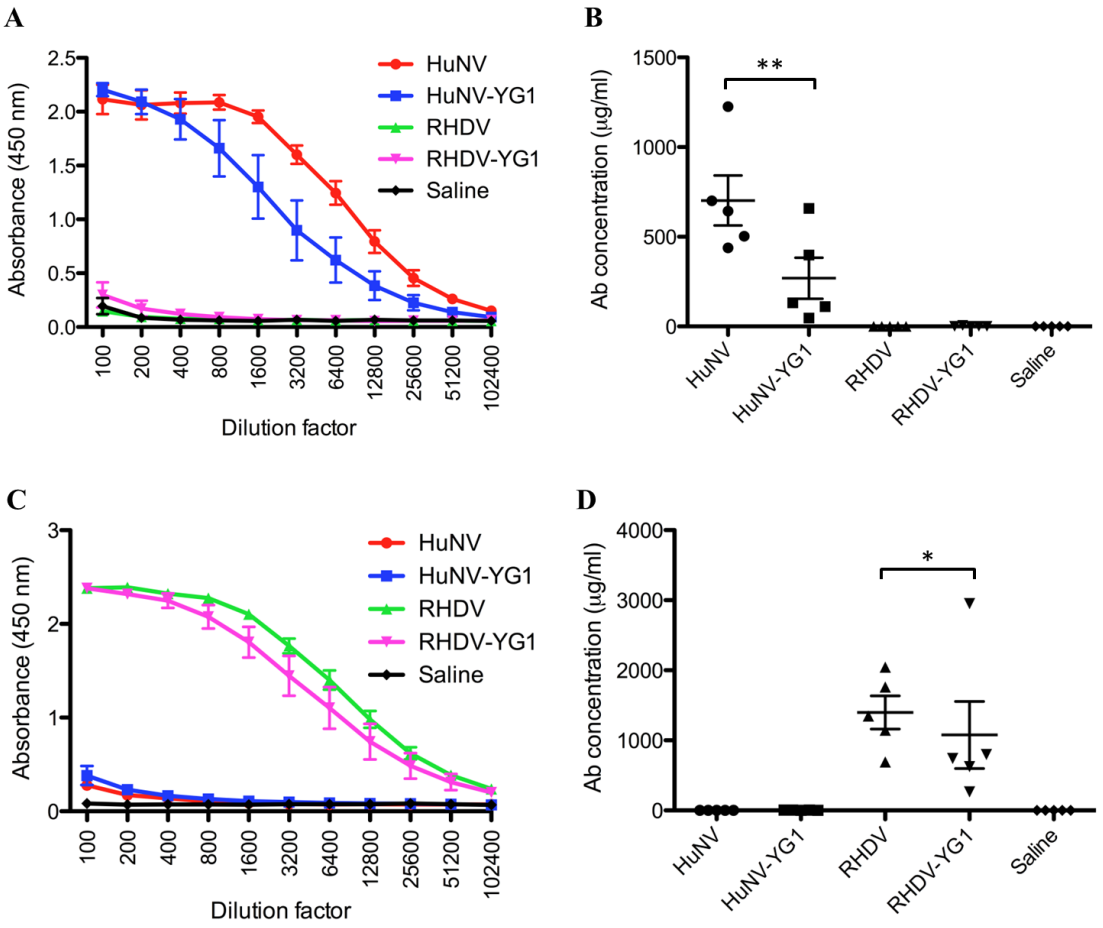

Figure 15. Serum IgG antibody responses to HuNV and RHDV VLP generated by VLP vaccinations

A) Titration curve of HuNV VLP-specific IgG antibody generated by vaccination with recombinant VLP, where dilutions are serial two-fold dilutions starting at 1 in 100. **B)** Concentration of IgG antibody specific for HuNV in the serum of vaccinated rats, with each symbol representing an individual animal and vaccination regime along the X-axis. **C)** Titration curve of RHDV VLP-specific IgG antibody generated by vaccination with recombinant VLP, where dilutions are serial two-fold dilutions starting at 1 in 100. **D)** Concentration of IgG antibody specific for RHDV in the serum of vaccinated rats, with each symbol representing an individual animal and vaccination regime along the X-axis. Data shown as mean ± SEM. * $p > 0.05$ calculated by a two-tailed, unpaired student's t-test, ** $p < 0.05$ calculated by a two-tailed, unpaired student's t-test

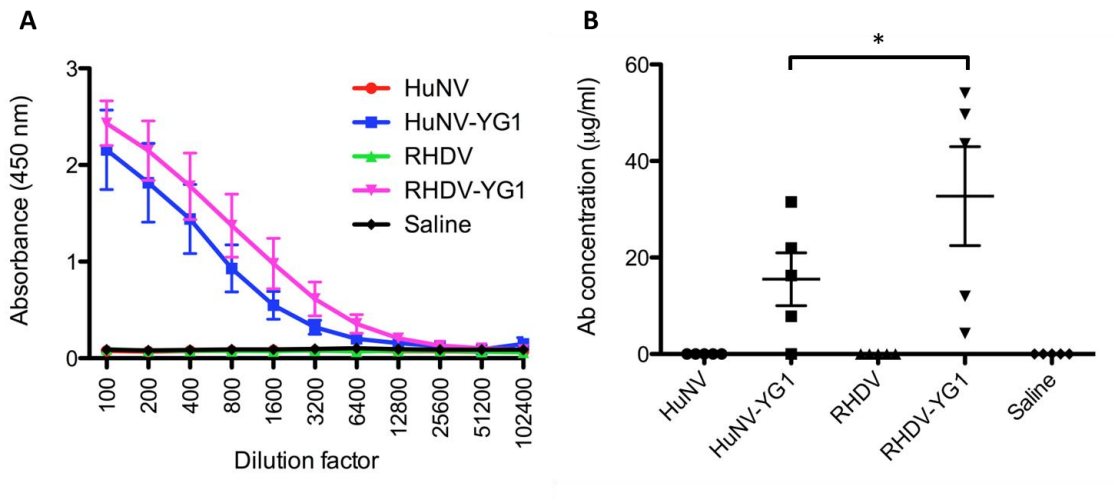

Figure 16. Serum IgG antibody response to YG1 generated by VLP vaccinations

A) Titration curve of YG1-specific IgG antibody generated by vaccination with recombinant VLP, where dilutions are serial two-fold dilutions starting at 1 in 100. **B)** Concentration of IgG antibody specific for YG1 in the serum of vaccinated rats, with each symbol representing an individual animal and vaccination regime along the X-axis. Data shown as mean ± SEM.. * $p > 0.05$ calculated by a two-tailed, unpaired student's t-test.

3.6.2 IgA in serum

Similar to IgG in serum, rats vaccinated with HuNV or RHDV derived VLP generated IgA against the VLP. All rats vaccinated with native HuNV VLP generated IgA antibodies in the serum against HuNV (Figure 17A), with an average titre of 7 µg/ml (Figure 17B), while four of the five rats vaccinated with HuNV-YG1.306 generated antibodies (Figure 17A), at an average titre of 4.5 µg/ml (Figure 17B). Likewise, all rats vaccinated with RHDV or RHDV-YG1.306 VLP elicited IgA antibody responses to RHDV VLP (Figure 17C), with an average titre of 28 µg/ml for those vaccinated with RHDV and 17 µg/ml for rats vaccinated with RHDV-YG1.306 (Figure 17D). Two out of five HuNV-YG1.368 vaccinated rats generated IgA antibodies against the YG1 peptide (Figure 18A), with an average titre of 373 ng/ml (Figure 18B), along with three of the five rats vaccinated with RHDV-YG1.306 (Figure 18A) at an average titre of 424 ng/ml (Figure 18B).

3.6.3 IgG and IgA in lung lavage

Analysis of carrier specific antibodies in lung lavage samples was not performed due to limited sample volumes. Small amounts of YG1 specific IgG were detected in two of the five rats vaccinated with HuNV-YG1.368 (Figure 19A), with titres only reaching 20 ng/ml (Figure 19B), while four out of five rats challenged with RHDV-YG1.306 generated YG1 specific IgG (Figure 19A), with an average titre of 168 ng/ml (Figure 19B). IgA antibodies specific for YG1 were not detected in significant levels in any of the vaccinated rat lung samples (Figure 19C & D).

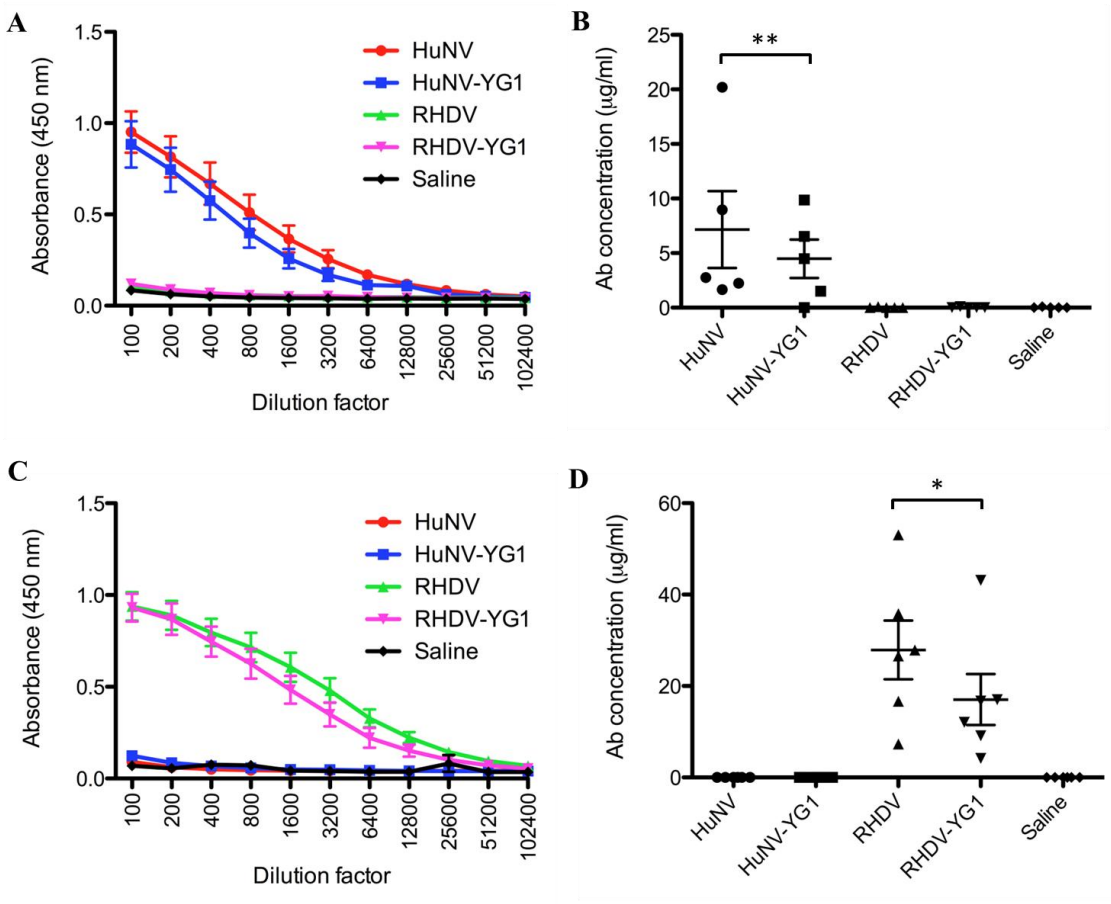

Figure 17. Serum IgA antibody responses to HuNV and RHDV VLP generated by VLP vaccinations

A) Titration curve of HuNV VLP-specific IgA antibody in serum generated by vaccination with recombinant VLP, where dilutions are serial two-fold dilutions starting at 1 in 100. **B)** Concentration of IgA antibody specific for HuNV in the serum of vaccinated rats, with each symbol representing an individual animal and vaccination regime along the X-axis. **C)** Titration curve of RHDV VLP-specific IgA antibody generated by vaccination with recombinant VLP, where dilutions are serial two-fold dilutions starting at 1 in 100. **D)** Concentration of IgA antibody specific for RHDV in the serum of vaccinated rats, with each symbol representing an individual animal and vaccination regime along the X-axis. Data shown as mean ± SEM. * $p > 0.05$ calculated by a two-tailed, unpaired student's t-test, ** $p < 0.05$ calculated by a two-tailed, unpaired student's t-test

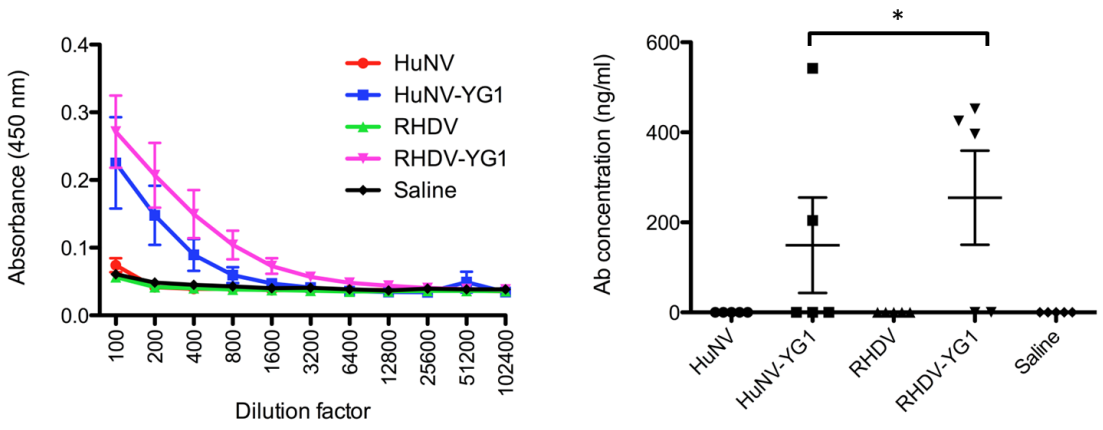

Figure 18. Serum IgA antibody response to YG1 peptide generated by VLP vaccination

A) Titration curve of YG1-specific IgA antibody generated by vaccination with recombinant VLP, where dilutions are serial two-fold dilutions starting at 1 in 100. **B)** Concentration of IgA antibody specific for YG1 in the serum of vaccinated rats, with each symbol representing an individual animal and vaccination regime along the X-axis. Data shown as mean ± SEM.. * $p > 0.05$ calculated by a two-tailed, unpaired student's t-test.

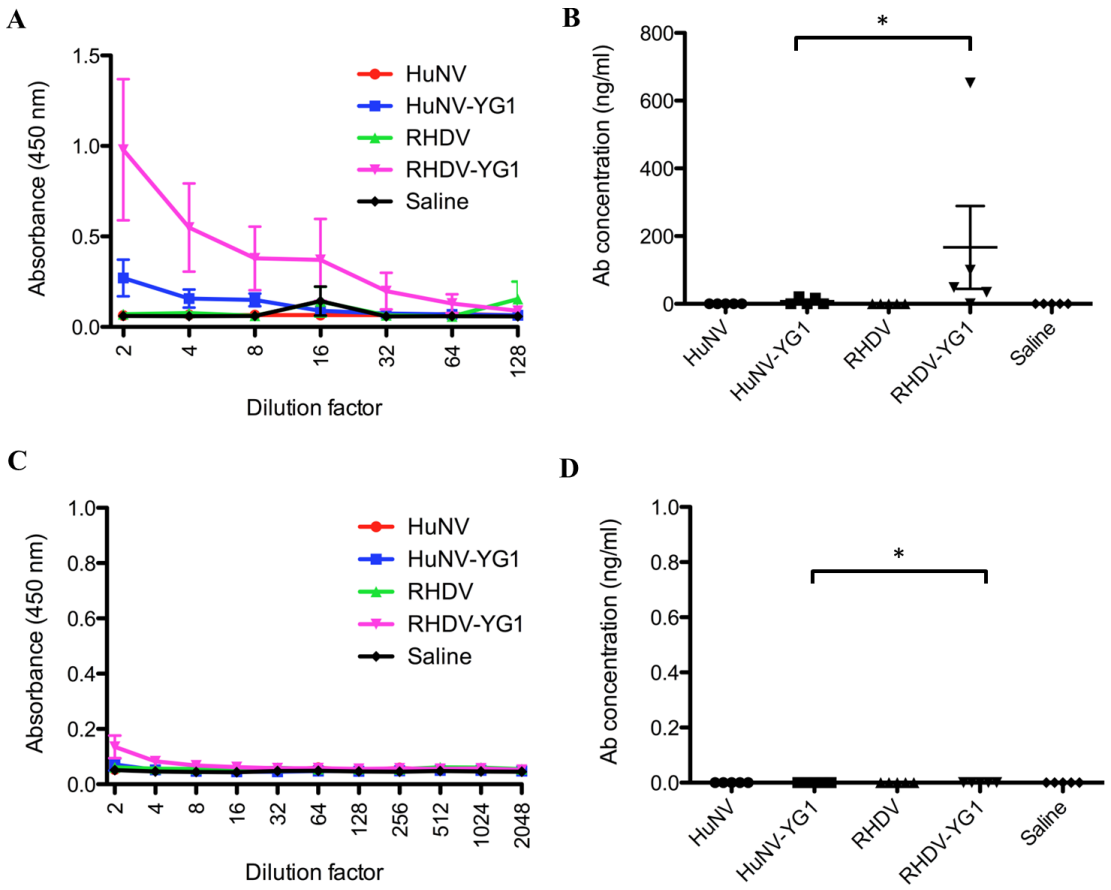

Figure 19. Lung lavage antibody responses to YG1 peptide generated by VLP vaccination

A) Titration curve of YG1 specific IgG antibody in lung lavage samples generated by vaccination with recombinant VLP, where dilutions are serial two-fold dilutions starting at 1 in 2. **B)** Concentration of IgG antibody specific for YG1 in the lungs of vaccinated rats, with each symbol representing an individual animal and vaccination regime along the X-axis. **C)** Titration curve of YG1 specific IgA antibody in lung lavage samples generated by vaccination with recombinant VLP, where dilutions are serial two-fold dilutions starting at 1 in 2. **D)** Concentration of IgA antibody specific for YG1 in the lungs of vaccinated rats, with each symbol representing an individual animal and vaccination regime along the X-axis. Data shown as mean ± SEM. * $p > 0.05$ calculated by a two-tailed, unpaired student's t-test

3.7 C-terminal modifications

Due to poor assembly of RHDV-YG1.306 VLP, an alternative insertion site was trialled. The YG1 epitope was inserted into the C-terminus of both VP58 and VP60 (Figure 10C & D). PCR of pFastBac/VP58 using the primer pair HuNV.VLPF and VP58-YG1.C-TERM and PCR of pAcpol$^-$/VP60-SL using the primer pair VP60F and VP60-YG1.C-TERM produced products of sizes 1675 and 1815, respectively, confirmed on a 1% agarose gel (Figure 20). The expected sequence of each gene was confirmed by sequencing. The recombinant genes were ligated into the transfer vector pAcpol$^-$ to form pAcpol$^-$/HUNV-YG1.CTERM and pAcpol$^-$/RHDV-YG1.CTERM (Figure 20)

Modified capsid genes were expressed in 50 ml insect cell cultures and purified by differential centrifugation. Assembly of C-terminally modified VLP was confirmed by T.E.M. Stable particles were seen from RHDV-YG1.CTERM (Figure 13D) but not from HUNV-YG1.CTERM.

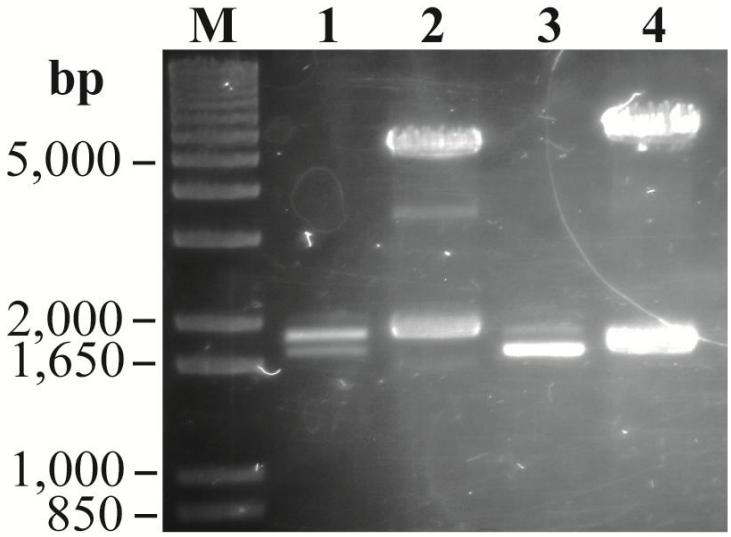

Figure 20. Construction of capsid genes including the YG1 epitope at their C-terminus

PCR was used to produce HuNV-YG1.CTERM and RHDV-YG1.CTERM. (1): HuNV-YG1.CTERM PCR product, 1675 bp, (2): full length modified capsid gene in the pAcpol$^-$ vector, digested with BamHI and EcoRI, (2): RHDV-YG1.CTERM PCR product, 1815 bp, (2): full length modified capsid gene in the pAcpol$^-$ vector, digested with BglII and EcoRI, (M) 1kb plus ladder marker.

4. Discussion

4.1 Capsid protein structure

The structures of HuNV VP58 and RHDV VP60 were analysed by iTASSER and Protean 3D. The structure of VP58, which has been determined by x-ray crystallography (49), was viewed using Protean 3D, whilst the structure of VP60 was predicated by iTASSER before being viewed using Protean 3D. The structures were used to analyse potential sites of epitope insertion within the P domain. Based on the literature, amino acid positions 368 for HuNV VP58 and 306 for RHDV VP60 were chosen as the most suitable for epitope insertion (10, 25). These sites locate to the P2 domain of the capsid genes. Inclusion of YG1 in the P2 domain was predicted to allow surface display of the epitope on the VLP, allowing the epitope to be processed as an extracellular antigen by the immune system and thus stimulate an antibody response.

4.2 Modification of viral capsid genes

VP58 and VP60 capsid proteins were modified to include the model antigen YG1 epitope of hTNF-α at a site predicted to locate to the P domain. The 14 amino acid YG1 sequence is smaller than the 15 and 17 amino acid sequences previously inserted into HuNV and RHDV VLP respectively (10, 25), thus both VLP were expected to tolerate the insertion without disruption of assembly. Each recombinant capsid gene included a glycine and serine residue (GS) on either side of the epitope. These residues act as flexible linkers to increase the malleability of YG1, promoting correct protein conformation (20).

The capsid genes were modified by PCR and subsequently the sequence was confirmed by the Massey Genome Service. The RHDV-YG1.306 gene showed both YG1 insertion and correct nucleotide sequence of the capsid protein. The HuNV-YG1.368 gene showed successful YG1 insertion, however the sequence did not match the full expected VP58 nucleotide sequence. A guanine-adenine substitution mutation was found which resulted in a change in amino acids at position 340 from a nonpolar alanine to a polar threonine. It was not known if this single substitution in primary structure will have any downstream consequences on the protein such as altering formation of the capsid protein, protein-protein interactions or solubility, which could impact the ability to form VLP. Single amino acid changes resulting in incorrect protein conformation are well characterised, such as the change in haemoglobin which results

in sickle cell anaemia (47). If the change at amino acid 340 did not result in prevention of VLP formation, the original sequence at this site can be assumed to not be essential for VLP assembly, meaning this location has some degree of flexibility and could be trialled as another site of insertion. Regardless, this construct was continued with due to time constraints.

4.3 Production, purification and analysis of VLP

Recombinant baculoviruses expressing the modified capsid genes were used to infect insect cells leading to the production of the modified proteins, which self-assembled into VLP. The baculovirus expression system was used due to the potential for eukaryotic post-translational modification and high yields of VLP (59). Differential centrifugation was used to separate the VLP from the cellular debris following treatment of the cell culture with Triton-X 100 to lyse the cell. Modified VLP were expected to be retained in the 10,000 x g supernatant to then pellet at 100,000 x g. RHDV-YG1.306 did not act as expected through the centrifugation, as it completely pelleted with the cellular debris during the 10,000 x g spin. We proposed that this was due to the capsid proteins not assembling correctly into stable particles, thus forming aggregates which were large enough to pellet at 10,000 x g.

Negatively stained VLP were analysed by T.E.M to confirm particle assembly. The distinctive VLP structures were visualised in high numbers in HuNV.YG1.368 samples. Whilst RHDV-YG1.306 VLP were visualised, they were only seen in very low numbers. The images indicated that while some VLP assembled, most of the protein was held as aggregates, explaining the unexpected results of centrifugation. We believe that the steric hindrance of the YG1 epitope at position 306 of VP60 prevented formation of stable VLP, allowing the capsid proteins to form random aggregates.

BCA assays were used to determine VLP concentration. Yields of HuNV-YG1.368 ranged from 1-2 mg per 400 ml culture, which is consistent with native HuNV VLP yields generated previously from our lab. The purity of the protein was low, with SDS-PAGE gels showing smaller protein bands at low concentrations. Although this is also consistent with previous HuNV VLP production, where protein degradation and “stickiness” of the VLP brings unwanted non-VLP proteins through the purification process, the purity of the recombinant HuNV VLP was much less than native HuNV.

Previous work from our lab has suggested that yields and purity of HuNV VLP can be improved by adding protease inhibitors when infecting the insect cell cultures, which could be a method to try with the recombinant VLP. Yields of RHDV-YG1.306 were low, at 0.5-2 mg per 400 ml culture, compared to expression and purification of native RHDV VLP in our lab yields of 8-10 mg of VLP per 400 ml culture. The modified protein was also much less pure than the native VLP, which was to be expected due to the alternate purification protocol used.

We have confirmed a suitable location in the structure of the HuNV VLP for insertion of an epitope of at least 14 amino acids. This site could have a range of implications for the continuing use of VLP in immunotherapeutics. Coupling sites could be included at this site, which could allow for specific peptides to be coupled straight onto the VLP without the need for a sulfo-SMCC linker (44). A purification tag, such as a polyhistidine-tag (His-tag), could be inserted on the surface of the VLP enabling purification by affinity chromatography. This would be especially useful for HuNV VLP purification due to the inherent impurity of VLP purified by current methods. Insertion of alternative epitopes would have to be trialled because a different amino acid sequences, even of the same size, may have different consequences on protein conformation.

Our results suggest that position 306 of RHDV VP60 is not a suitable site for peptide insertion without interrupting VLP assembly. It is interesting that the results of this study were not consistent with results gathered by Crisci *et al.* (2009), as the epitope we used was smaller than the epitope they were able to insert into RHDV VLP. This could be explained by differences in the chemical or steric properties of each peptide. Estimation of the charge of each peptide using Protein Calculator v3.3 (Scripps Research Institute) indicated that the YG1 peptide has an overall positive charge while the epitope used by Crisci *et al.* (2009) had an overall negative charge. It is possible that positively charged YG1 peptide is more obstructive to VP60 tertiary structure, interrupting spontaneous VLP formation. Regardless, the use of position 306 for peptide insertion would appear to be peptide specific. Insertion of the YG1 peptide could be trialled at alternate locations within the P2 domain to find a surface loop which is more universally accepting of peptides. Also, in an attempt to find an alternative to recombinant RHDV VLP, the recombinant P domain alone could be

expressed in insect cells to see if it will assemble into P particles, as the HuNV VP58 P domain does (54, 56).

4.4 Antibody responses to modified VLP

Rats were vaccinated with either HuNV, HuNV-YG1.368, RHDV or RHDV-YG1.306 VLP, or saline, depending on vaccination group. YG1 peptide alone was not used as a vaccination group as peptides have been shown to be poorly immunogenic, and general practice is to couple peptides to carriers (19). ELISA assays were used to quantify the specific IgG and IgA antibody responses to the HuNV and RHDV carriers, and the inserted YG1 epitope in all vaccinated rats.

As expected, results from these assays showed that all VLP vaccinated rats generated serum IgG antibodies against the VLP from which the vaccine was derived. For example, HuNV specific IgG was detected in the serum of all rats vaccinated with either native HuNV or HuNV-YG1.368 VLP and likewise for native and recombinant RHDV. This shows that the inserted epitope did not prevent the generation of antibodies to the parent VLP. This was expected for modified HuNV, as the VLP did not have trouble assembling and thus would have resembled native HuNV. However it was interesting that the same was found for modified RHDV. This was unexpected as RHDV-YG1.306 was not efficiently forming stable particles and most the protein was aggregating into random masses, probably due to incorrect protein conformation, which should impede its ability to generate antibodies to the correctly formed particles. What we observed could be explained by us underestimating the ability of RHDV-YG1.306 to form VLP, or that the conformation differences did not significantly alter the capsid protein epitopes despite preventing assembly. Due to the small volumes of lung lavage sample obtained, antibodies specific for the two VLP carriers could not be analysed in these samples.

The measured antibody responses to VLP carriers may not be fully indicative of VLP specific antibodies. It is important to consider that both the vaccine preparations and VLP used to coat ELISA plates were produced in insect cells, and consequently would likely both contain insect cell debris. It is feasible that rats vaccinated against VLP also generated antibodies against the cellular debris, which would be detected by binding of said antibodies to debris in the VLP samples used to coat the ELISA plates. Thus,

responses seen against the VLP were realistically responses towards VLP and, to a lesser extent, insect cells.

Specific antibodies to YG1 were detected in the serum of rats vaccinated with recombinant VLP. Four of the five rats vaccinated with HuNV-YG1.368 and all five rats vaccinated with RHDV-YG1.306 generated IgG specific for the YG1 peptide. This important result tells us that the YG1 epitope we inserted into each capsid protein was available for immune recognition. The epitope could have been buried deep enough within the structure of the VLP or protein to make it difficult to recognise or cleave from the protein. These results also confirm that the YG1 epitope was present in the modified RHDV particles, which was not confirmed by mass spectrometry results. Specific antibodies to YG1 were also detected in the lung lavage samples of vaccinated rats. RHDV-YG1.306 was able to effectively generate IgG in the lung, while HuNV-YG1.368 generated some mucosal IgG but at very low concentrations. Only a low level of IgG in the lungs was to be expected as this is not the major type of antibody present in the lungs; however lung lavage samples are not as confirmative as serum samples due to the difficulty and potential for variation during collection.

An important aim of this project was to determine whether recombinant VLP are able to stimulate equal IgG responses against the YG1 epitope as when the epitope was coupled to VLP. To determine this, serum from rats vaccinated with coupled HuNV-YG1 and RHDV-YG1 (Sam McClintock, BSc(Hons) project) was analysed in parallel with serum from this study (Appendix 2). This showed that YG1 coupled to HuNV stimulated a 10-fold greater immune response than the recombinant HuNV VLP, while the two RHDV VLPs were not substantially different. The difference in the HuNV vaccinated rats could be explained by the availability of the YG1 epitope to the rat immune system. When coupled to a VLP, an epitope extends from the surface of the VLP by the Sulfo-SMCC linker. When the epitope is genetically inserted into the capsid gene, it is embedded into the structure of the protein. This makes it less available for recognition by the immune system and more difficult to cleave out of the protein than the coupled version, meaning less of the antigen gets presented via MHC molecules. However despite the disadvantages with coupling, there is no point switching to recombinant VLP if coupled VLP generate stronger immune responses.

In addition to IgG, specific IgA antibodies against the VLP carriers and the YG1 peptide were analysed in the serum, and lung lavage samples analysed for YG1 specific IgA. Similar trends seen for serum IgG were seen for IgA antibodies in the serum specific for YG1 and the two VLP carriers, albeit at much lower titres than IgG. IgA could not be detected at significant levels in any of the lung samples. This is consistent with data from our lab, which suggests that stimulation of an IgA mucosal immune response requires a mucosal adjuvant such as Gardiquimod™. Gardiquimod™ is a TLR7 agonist, which is important in activating a T-helper 1 (Th1) cell mediated immunity (64). Research has shown that this type of Th1 immunity is essential for antibody isotype switching (60), resulting in production of the secretory form of IgA which is the most abundant mucosal antibody (9). Isotype switching is essential for production of the dimeric secretory form of IgA but not the monomeric form found in serum, explaining why IgA was detected in the serum but not lung. However, uncertainties must be accounted for when analysing lung samples due to the difficulty and variations with lung lavage. Liquid used for lavage may be lost within the animal due to lung punctures or poor technique and it is never known by how much the mucosal antibodies have been diluted when the sample is retrieved.

Taken together, the antibody response results show that the recombinant VLP developed in this study have the potential for use as a dual target vaccine, targeting both the parent virus and the inserted epitope. As mentioned previously, a desired epitope of the same size would have to be trialled due to differences in amino acid structure that may lead to variation in capsid protein folding.

The use of two types of VLP in this study was significant as it allows for an alternating carrier prime boost vaccine schedule to be used, such as recombinant HuNV as the prime and recombinant RHDV for the boost. Previous work from our lab has suggested that carrier-specific pre-existing antibodies generated from the prime vaccine clear the VLP in the boost vaccine, reducing the effectiveness of the booster immunization (Sam McClintock, BSc(Hons), 2011). This phenomenon is known as carrier induced epitopic suppression (CIES) (26). Using different modified VLP for the prime and boost vaccines may prevent this phenomenon and improve the overall antibody response generated to the antigen. Similar results have been found where native HPV antibodies reacted against chimeric HPV carrying the E7 protein, preventing the immune response against E7 from being effective (13). Conversely, the use of the same carrier for each

vaccine may allow carrier specific antibodies generated by the prime vaccine to opsonise the boost vaccine VLP, increasing the uptake of the VLP into APCs. These theories will have to be studied in depth before meaningful conclusions can be drawn.

An interesting trend from this study was that the RHDV-YG1.306 vaccine was more effective at generating both IgA and IgG antibodies than HuNV-YG1.368, although there was no overall statistically significant difference. The fact that the RHDV derived protein did not form stable structures made us think that a trend in the opposite direction would be seen. A possible explanation could be found in the purification procedure, where the RHDV derived protein was essentially a crude cell lysate of aggregated protein, compared to the more purified, organised HuNV product. Insect cell debris from crude cell lysates could act as an adjuvant, improving the immune response to the desired antigen.

4.5 C-terminal modifications

Due to difficulties in RHDV-YG1.306 VLP formation, an alternative insertion site was trialled. The YG1 antigen was included at the C-terminus of both VP58 and VP60 capsid proteins. This site locates to outer regions of the P1 domain, meaning this region has potential for the surface display of peptides without interrupting protein folding. These genes were produced to determine whether the C-terminus is suitable for epitope insertion however the resulting VLP were not to be used in vaccination. Both genes included a GS residue on the N-terminal side of the epitope to aid correct protein folding.

T.E.M analysis of the purified C-terminally modified VLP showed that RHDV-YG1.CTERM efficiently assembled into stable particles, where HuNV-YG1.CTERM did not. RHDV assembly is consistent with results from Nagesha *et al.* (1999) (41), however there are no published reports of inclusion of an epitope at the C-terminus of HuNV VP58. No immunogenicity data was gathered from RHDV-YG1.CTERM, however it could act as an alternative to RHDV-YG1.306.

4.6 Conclusions

In summary, recombinant HuNV and RHDV VLP can be generated by engineering a peptide to be displayed on the surface of the VLP. Electron microscopy was used to

visualise assembled VLP and mass spectrometry used to confirm YG1 epitope insertion. Vaccination of rats with modified VLP with YG1 on the surface generated IgG and IgA in the serum against both the carrier and the YG1 epitope, whilst only small amounts of IgG and no IgA was detected in the lungs.

In this study we have successfully confirmed a suitable position to insert an antigen on the surface of HuNV VLP, which could be used for vaccination, coupling or purification. Our recombinant HuNV was able to generate antibodies against both the carrier and the inserted epitope. Insertion into the surface of RHDV VLP was questionable, where only a few VLP were seen and much of the protein formed aggregates. Despite this, the recombinant RHDV was able to generate antibodies against both the carrier and the inserted epitope. Inclusion of an epitope at the C-terminus of HuNV VP58 did not generate VLP, whereas inclusion at the C-terminus of RHDV VP60 did. No immunogenicity data was collected, thus this VLP should be trialled to determine its effectiveness as a vaccine carrier.

4.7 Future directions

Our results concerning the assembly of RHDV-YG1.306 are not consistent with a previous study by Crisci *et al.* (2009). They achieved higher yields and assembly of their modified RHDV VLP with a surface insertion than we could achieve. This could be simply due to the amino acid structure of the peptide they used, which may have been more amenable to insertion at position 306 due to amino acid charges, polarity or steric hindrance. Adding further flexible amino acids to the glycine serine linkers (e.g. $(GGGS)_n$) on each side of the epitope may improve the stability and conformation of the particles. Insertion of alternate epitopes at the same site would allow further insight into the receptiveness of position 306 for epitope insertion. A more in-depth analysis of RHDV-YG1.CTERM could also uncover a more effective vaccination candidate to replace the surface version.

HuNV VLP was seen to tolerate the insertion at amino acid position 368; however yields and purity of the VLP were low. Optimising the production and purification of the VLP could lead to improvement to these two variables, such as addition of protease inhibitors during protein expression or use of alternative detergents during purification to prevent aggregation. In this study, Tween-20 was added to each step during

purification at a concentration of 0.01%, however recent optimisation of native HuNV VLP purification in our lab has shown than the same concentration of Triton-X is far more effective, increasing both yield and purity (Sarah Scullion, personal communication). Such optimisation could lead to similar findings for HuNV-YG1.368.

5. References

1. **Abrantes, J., W. van der Loo, J. Le Pendu, and P. Esteves.** 2012. Rabbit haemorrhagic disease (RHD) and rabbit haemorrhagic disease virus (RHDV): a review. Veterinary Research **43:**12.

2. **Ackerman, A. L., and P. Cresswell.** 2004. Cellular mechanisms governing cross-presentation of exogenous antigens. Nature Immunology **5:**678-684.

3. **Anderson, E. L., D. J. Kennedy, K. M. Geldmacher, J. Donnelly, and P. M. Mendelman.** 1996. Immunogenicity of heptavalent pneumococcal conjugate vaccine in infants. The Journal of Pediatrics **128:**649-653.

4. **Andre, F. E., and A. Safary.** 1987. Summary of clinical findings on Engerix-B, a genetically engineered yeast derived hepatitis B vaccine. Postgraduate medical journal **63 Suppl 2:**169-177.

5. **Baba, T. W., V. Liska, A. H. Khimani, N. B. Ray, P. J. Dailey, D. Penninck, R. Bronson, M. F. Greene, H. M. McClure, L. N. Martin, and R. M. Ruprecht.** 1999. Live attenuated, multiply deleted simian immunodeficiency virus causes AIDS in infant and adult macaques. Nature medicine **5:**194-203.

6. **Bellier, B., C. Dalba, B. Clerc, D. Desjardins, R. Drury, F. L. Cosset, M. Collins, and D. Klatzmann.** 2006. DNA vaccines encoding retrovirus-based virus-like particles induce efficient immune responses without adjuvant. Vaccine **24:**2643-2655.

7. **Boga, J. A., R. Casais, M. S. Marin, J. M. Martin-Alonso, R. S. Carmenes, M. Prieto, and F. Parra.** 1994. Molecular cloning, sequencing and expression in Escherichia coli of the capsid protein gene from rabbit haemorrhagic disease virus (Spanish isolate AST/89). The Journal of general virology **75:**2409-2413.

8. **Boga, J. A., J. M. Mart√≠n Alonso, R. Casais, and F. Parra.** 1997. A single dose immunization with rabbit haemorrhagic disease virus major capsid protein produced in Saccharomyces cerevisiae induces protection. Journal of General Virology **78:**2315-2318.

9. **Corthesy, B.** 2010. Role of secretory immunoglobulin A and secretory component in the protection of mucosal surfaces. Future Microbiol **5:**817-829.

10. **Crisci, E., H. Almanza, I. Mena, L. Cordoba, E. Gomez-Casado, J. R. Caston, L. Fraile, J. Barcena, and M. Montoya.** 2009. Chimeric calicivirus-like particles elicit protective anti-viral cytotoxic responses without adjuvant. Virology **387:**303-312.

11. **Crisci, E., L. Fraile, N. Moreno, E. Blanco, R. Cabezón, C. Costa, T. Mussá, M. Baratelli, P. Martinez-Orellana, L. Ganges, J. Martínez, J. Bárcena, and M. Montoya.** 2012. Chimeric calicivirus-like particles elicit specific immune responses in pigs. Vaccine **30:**2427-2439.

12. **Cubas, R., S. Zhang, S. Kwon, E. M. Sevick-Muraca, M. Li, C. Chen, and Q. Yao.** 2009. Virus-like particle (VLP) lymphatic trafficking and immune response generation after immunization by different routes. Journal of immunotherapy **32:**118-128.

13. **Da Silva, D. M., D. V. Pastrana, J. T. Schiller, and W. M. Kast.** 2001. Effect of Preexisting Neutralizing Antibodies on the Anti-tumor Immune Response Induced by Chimeric Human Papillomavirus Virus-like Particle Vaccines. Virology **290:**350-360.

14. **Dong, J., Y. Gao, Y. Liu, J. Shi, J. Feng, Z. Li, H. Pan, Y. Xue, C. Liu, B. Shen, N. Shao, and G. Yang.** 2010. The Protective Antibodies Induced by a Novel Epitope of Human TNF-α Could Suppress the Development of Collagen-Induced Arthritis. PLoS ONE **5:**e8920.

15. **Dyson, N., P. Guida, K. Munger, and E. Harlow.** 1992. Homologous sequences in adenovirus E1A and human papillomavirus E7 proteins mediate interaction with the same set of cellular proteins. Journal of virology **66:**6893-6902.

16. **El Mehdaoui, S., A. Touze, S. Laurent, P. Y. Sizaret, D. Rasschaert, and P. Coursaget.** 2000. Gene transfer using recombinant rabbit hemorrhagic disease virus capsids with genetically modified DNA encapsidation capacity by addition of packaging sequences from the L1 or L2 protein of human papillomavirus type 16. Journal of virology **74:**10332-10340.

17. **Escribano, J. M., and D. M. Perez-Filgueira.** 2009. Strategies for Improving Vaccine Antigens Expression in Transgenic Plants: Fusion to Carrier Sequences:

Recombinant Proteins From Plants, p. 275-287. *In* L. Faye and V. Gomord (ed.), vol. 483. Humana Press.

18. **Fifis, T., A. Gamvrellis, B. Crimeen-Irwin, G. A. Pietersz, J. Li, P. L. Mottram, I. F. C. McKenzie, and M. Plebanski.** 2004. Size-Dependent Immunogenicity: Therapeutic and Protective Properties of Nano-Vaccines against Tumors. The Journal of Immunology **173:**3148-3154.

19. **Foged, C.** 2011. Subunit vaccines of the future: the need for safe, customized and optimized particulate delivery systems. Therapeutic delivery **2:**1057-1077.

20. **Freund, C., A. Ross, B. Guth, A. Pluckthun, and T. A. Holak.** 1993. Characterization of the linker peptide of the single-chain Fv fragment of an antibody by NMR spectroscopy. FEBS letters **320:**97-100.

21. **Garcea, R. L., and L. Gissmann.** 2004. Virus-like particles as vaccines and vessels for the delivery of small molecules. Current Opinion in Biotechnology **15:**513-517.

22. **Glass, R. I., U. D. Parashar, and M. K. Estes.** 2009. Norovirus Gastroenteritis. New England Journal of Medicine **361:**1776-1785.

23. **Guermonprez, P., J. Valladeau, L. Zitvogel, C. Théry, and S. Amigorena.** 2002. Antigen presentation and T cell stimulation by dendtitic cells. Annual Review of Immunology **20:**621-667.

24. **Hanley, K. A.** 2011. The double-edged sword: How evolution can make or break a live-attenuated virus vaccine. Evolution **4:**635-643.

25. **Herbst-Kralovetz, M., H. S. Mason, and Q. Chen.** 2010. Norwalk virus-like particles as vaccines. Expert Rev Vaccines **9:**299-307.

26. **Jegerlehner, A., M. Wiesel, K. Dietmeier, F. Zabel, D. Gatto, P. Saudan, and M. F. Bachmann.** 2010. Carrier induced epitopic suppression of antibody responses induced by virus-like particles is a dynamic phenomenon caused by carrier-specific antibodies. Vaccine **28:**5503-5512.

27. **Jiang, X., M. Wang, D. Y. Graham, and M. K. Estes.** 1992. Expression, self-assembly, and antigenicity of the Norwalk virus capsid protein. Journal of virology **66:**6527-6532.

28. **Joffre, O. P., E. Segura, A. Savina, and S. Amigorena.** 2012. Cross-presentation by dendritic cells. Nat Rev Immunol **12:**13.

29. **Katpally, U., N. R. Voss, T. Cavazza, S. Taube, J. R. Rubin, V. L. Young, J. Stuckey, V. K. Ward, H. W. t. Virgin, C. E. Wobus, and T. J. Smith.** 2010. High-resolution cryo-electron microscopy structures of murine norovirus 1 and rabbit hemorrhagic disease virus reveal marked flexibility in the receptor binding domains. Journal of virology **84:**5836-5841.

30. **Keating, G. M., and S. Noble.** 2003. Recombinant Hepatitis B Vaccine (Engerix-B(R)): A Review of its Immunogenicity and Protective Efficacy Against Hepatitis B. Drugs **63:**1021-1051.

31. **Klamp, T., J. Schumacher, G. Huber, C. Kuhne, U. Meissner, A. Selmi, T. Hiller, S. Kreiter, J. Markl, O. Tureci, and U. Sahin.** 2011. Highly specific auto-antibodies against claudin-18 isoform 2 induced by a chimeric HBcAg virus-like particle vaccine kill tumor cells and inhibit the growth of lung metastases. Cancer research **71:**516-527.

32. **Laurent, S., J. F. Vautherot, M. F. Madelaine, G. Le Gall, and D. Rasschaert.** 1994. Recombinant rabbit hemorrhagic disease virus capsid protein expressed in baculovirus self-assembles into viruslike particles and induces protection. Journal of virology **68:**6794-6798.

33. **Lindesmith, L., C. Moe, S. Marionneau, N. Ruvoen, X. Jiang, L. Lindblad, P. Stewart, J. LePendu, and R. Baric.** 2003. Human susceptibility and resistance to Norwalk virus infection. Nature medicine **9:**548-553.

34. **Liu, F., S. Ge, L. Li, X. Wu, Z. Liu, and Z. Wang.** 2011. Virus-like particles: potential veterinary vaccine immunogens. Research in Veterinary Science **93:**553-559.

35. **Lo-Man, R., P. Rueda, C. Sedlik, E. Deriaud, I. Casal, and C. Leclerc.** 1998. A recombinant virus-like particle system derived from parvovirus as an efficient

antigen carrier to elicit a polarized Th1 immune response without adjuvant. European journal of immunology **28:**1401-1407.

36. **Luque, D., J. M. González, J. Gómez-Blanco, R. Marabini, J. Chichón, I. Mena, I. Angulo, J. L. Carrascosa, N. Verdaguer, B. L. Trus, J. Bárcena, and J. R. Castón.** 2012. Epitope Insertion at the N-Terminal Molecular Switch of the Rabbit Hemorrhagic Disease Virus T=3 Capsid Protein Leads to Larger T=4 Capsids. Journal of virology **86:**6470-6480.

37. **Mandl, S., L. J. Sigal, K. L. Rock, and R. Andino.** 1998. Poliovirus vaccine vectors elicit antigen-specific cytotoxic T cells and protect mice against lethal challenge with malignant melanoma cells expressing a model antigen. Proceedings of the National Academy of Sciences **95:**8216-8221.

38. **Markham, A., and H. M. Lamb.** 2000. Infliximab: A Review of its Use in the Management of Rheumatoid Arthritis. Drugs **59:**1341-1359.

39. **Matzelle, M. M., and J. E. Babensee.** 2004. Humoral immune responses to model antigen co-delivered with biomaterials used in tissue engineering. Biomaterials **25:**295-304.

40. **McAleer, W. J., E. B. Buynak, R. Z. Maigetter, D. E. Wampler, W. J. Miller, and M. R. Hilleman.** 1984. Human hepatitis B vaccine from recombinant yeast. Nature **307:**178-180.

41. **Nagesha, H. S., L. F. Wang, and A. D. Hyatt.** 1999. Virus-like particles of calicivirus as epitope carriers. Archives of Virology **144:**2429-2439.

42. **Nagesha, H. S., L. F. Wang, A. D. Hyatt, C. J. Morrissy, C. Lenghaus, and H. A. Westbury.** 1995. Self-assembly, antigenicity, and immunogenicity of the rabbit haemorrhagic disease virus (Czechoslovakian strain V-351) capsid protein expressed in baculovirus. Archives of Virology **140:**1095-1108.

43. **Osaki, F., T. Kanamori, S. Sando, T. Sera, and Y. Aoyama.** 2004. A Quantum Dot Conjugated Sugar Ball and Its Cellular Uptake. On the Size Effects of Endocytosis in the Subviral Region. Journal of the American Chemical Society **126:**6520-6521.

44. **Patel, K. G., and J. R. Swartz.** 2011. Surface Functionalization of Virus-Like Particles by Direct Conjugation Using Azide−Alkyne Click Chemistry. Bioconjugate Chemistry **22:**376-387.

45. **Peacey, M., S. Wilson, M. A. Baird, and V. K. Ward.** 2007. Versatile RHDV virus-like particles: Incorporation of antigens by genetic modification and chemical conjugation. Biotechnol Bioeng **98:**968-977.

46. **Pejawar-Gaddy, S., Y. Rajawat, Z. Hilioti, J. Xue, D. Gaddy, O. Finn, R. Viscidi, and I. Bossis.** 2010. Generation of a tumor vaccine candidate based on conjugation of a MUC1 peptide to polyionic papillomavirus virus-like particles. Cancer Immunology, Immunotherapy **59:**1685-1696.

47. **Powars, D., L. S. Chan, and W. A. Schroeder.** 1990. The variable expression of sickle cell disease is genetically determined. Seminars in hematology **27:**360-376.

48. **Prasad, B. V., M. E. Hardy, T. Dokland, J. Bella, M. G. Rossmann, and M. K. Estes.** 1999. X-ray crystallographic structure of the Norwalk virus capsid. Science (New York, N.Y.) **286:**287-290.

49. **Prasad, B. V. V., M. E. Hardy, T. Dokland, J. Bella, M. G. Rossmann, and M. K. Estes.** 1999. X-ray Crystallographic Structure of the Norwalk Virus Capsid. Science (New York, N.Y.) **286:**287-290.

50. **Prasad, B. V. V., D. O. Matson, and A. W. Smith.** 1994. Three-dimensional Structure of Calicivirus. Journal of Molecular Biology **240:**256-264.

51. **Santi, L., L. Batchelor, Z. Huang, B. Hjelm, J. Kilbourne, C. J. Arntzen, Q. Chen, and H. S. Mason.** 2008. An efficient plant viral expression system generating orally immunogenic Norwalk virus-like particles. Vaccine **26:**1846-1854.

52. **Scheffner, M., B. A. Werness, J. M. Huibregtse, A. J. Levine, and P. M. Howley.** 1990. The E6 oncoprotein encoded by human papillomavirus types 16 and 18 promotes the degradation of p53. Cell **63:**1129-1136.

53. **Suzich, J. A., S. J. Ghim, F. J. Palmer-Hill, W. I. White, J. K. Tamura, J. A. Bell, J. A. Newsome, A. B. Jenson, and R. Schlegel.** 1995. Systemic immunization

with papillomavirus L1 protein completely prevents the development of viral mucosal papillomas. Proceedings of the National Academy of Sciences **92:**11553-11557.

54. **Tan, M., P. Huang, M. Xia, P. A. Fang, W. Zhong, M. McNeal, C. Wei, W. Jiang, and X. Jiang.** 2011. Norovirus P particle, a novel platform for vaccine development and antibody production. Journal of virology **85:**753-764.

55. **Tan, M., and X. Jiang.** 2012. The formation of P particle increased immunogenicity of norovirus P protein. Immunology **136:**28-29.

56. **Tan, M., and X. Jiang.** 2005. The p domain of norovirus capsid protein forms a subviral particle that binds to histo-blood group antigen receptors. Journal of virology **79:**14017-14030.

57. **Tan, M., W. Zhong, D. Song, S. Thornton, and X. Jiang.** 2004. E. coli-expressed recombinant norovirus capsid proteins maintain authentic antigenicity and receptor binding capability. Journal of medical virology **74:**641-649.

58. **Tarp, M. A., and H. Clausen.** 2008. Mucin-type O-glycosylation and its potential use in drug and vaccine development. Biochimica et Biophysica Acta (BBA) - General Subjects **1780:**546-563.

59. **van Oers, M. M.** 2011. Opportunities and challenges for the baculovirus expression system. Journal of invertebrate pathology **107 Suppl:**S3-15.

60. **Velasquez, L. S., B. E. Hjelm, C. J. Arntzen, and M. M. Herbst-Kralovetz.** 2010. An intranasally delivered Toll-like receptor 7 agonist elicits robust systemic and mucosal responses to Norwalk virus-like particles. Clinical and vaccine immunology : CVI **17:**1850-1858.

61. **Villa, L. L., K. A. Ault, A. R. Giuliano, R. L. Costa, C. A. Petta, R. P. Andrade, D. R. Brown, A. Ferenczy, D. M. Harper, L. A. Koutsky, R. J. Kurman, M. Lehtinen, C. Malm, S. E. Olsson, B. M. Ronnett, F. E. Skjeldestad, M. Steinwall, M. H. Stoler, C. M. Wheeler, F. J. Taddeo, J. Yu, L. Lupinacci, R. Railkar, R. Marchese, M. T. Esser, J. Bryan, K. U. Jansen, H. L. Sings, G. M. Tamms, A. J. Saah, and E. Barr.** 2006. Immunologic responses following administration of a vaccine targeting human papillomavirus Types 6, 11, 16, and 18. Vaccine **24:**5571-5583.

62. **Wagner, R., V. J. Teeuwsen, L. Deml, F. Notka, A. G. Haaksma, S. S. Jhagjhoorsingh, H. Niphuis, H. Wolf, and J. L. Heeney.** 1998. Cytotoxic T cells and neutralizing antibodies induced in rhesus monkeys by virus-like particle HIV vaccines in the absence of protection from SHIV infection. Virology **245:**65-74.

63. **Watts, C.** 2004. The exogenous pathway for antigen presentation on major histocompatibility complex class II and CD1 molecules. Nature Immunology **5:**685-692.

64. **Wermuth, P. J., and S. A. Jimenez.** 2012. Gadolinium compounds signaling through TLR4 and TLR7 in normal human macrophages: establishment of a proinflammatory phenotype and implications for the pathogenesis of nephrogenic systemic fibrosis. J Immunol **189:**318-327.

65. **Win, S. J., V. K. Ward, P. R. Dunbar, S. L. Young, and M. A. Baird.** 2011. Cross-presentation of epitopes on virus-like particles via the MHC I receptor recycling pathway. Immunol Cell Biol **89:**681-688.

66. **Xia, M., T. Farkas, and X. Jiang.** 2007. Norovirus capsid protein expressed in yeast forms virus-like particles and stimulates systemic and mucosal immunity in mice following an oral administration of raw yeast extracts. Journal of medical virology **79:**74-83.

67. **Zhang, Z., M. A. Miteva, L. Wang, and E. Alexov.** 2012. Analyzing effects of naturally occurring missense mutations. Computational and mathematical methods in medicine **2012:**805827.

6. Appendices

Appendix 1. Recipes

Agarose Gels

50 x TAE buffer

242 g Tris

57 ml Glacial acetic acid

100 ml 0.5 M EDTA pH 8.0

Bring to 1000 ml with deionised water then autoclave

1% agarose gel

0.4 g Agarose

800 µl 50x TAE buffer

40 ml Deionised water

Heat in a microwave until all agarose is dissolved

Cool agarose with tap water

Poor agarose into cradle and allow 20-30 minutes to set

Gel loading dye

25 mg Bromophenol blue

2.5 g Ficoll-400

10 ml MillQ H_2O

Dilute 1 in 10 in millQ H_2O for loading

Ethidium bromide stain

100 µg Ethidium bromide

100 ml Deionised water

Mix thoroughly

VLP production and purification

LB broth

10 g	Bactotryptone
5 g	Bacto yeast extract
5 g	NaCl

Make up to 1000 ml with distilled water then autoclave

LB agar

15 g	Agar
10 g	Bactotryptone
5 g	Bacto yeast extract
5 g	NaCl

Make up to 1000 ml with distilled water then autoclave

VLP production and purification

Trypan blue

0.5 g	Trypan blue
10 ml	Milli-Q H_2O

Filter sterilise

Insect phosphate buffered saline (iPBS)

0.14 g	Na_2HPO_4
1.43 g	KH_2PO_4
8.18 g	NaCl
2.98 g	KCl

Make up to 1000 ml with distilled water then autoclave

CsCl gradient

1.4 g/cm^3 CsCl		1.2 g/cm^3 CsCl	
6.15 g	CsCl	2.86 g	CsCl
10 ml	Mili-Q H_2O	10 ml	Mili-Q H_2O

Filter sterilise

Underlay 3 ml of 1.2 g/cm^3 CsCl with 3 ml of 1.4 g/cm^3 CsCl in an ultracentrifuge tube

Pipette VLP sample on top of the gradient, then fill tube to the top with insect PBS

SDS-PAGE

Acrylamide

40% Acrylamide/Bis solution was used in all Acrylamide gel preparations.

Resolving gel buffer

0.4 g	SDS
18.2 g	Tris
70 ml	Milli-Q water

Adjust pH to 8.8 with HCl.

Bring volume to 100 ml with Milli-Q water.

Stacking gel buffer

0.4 g	SDS
6.04 g	Tris
70 ml	Milli-Q water

Adjust pH to 8.6 with HCl.

Bring volume to 100 ml with Milli-Q water.

One 12.5% acrylamide gel

Resolving gel		Stacking gel	
2.34 ml	40% Acrylamide	0.25 ml	40% Acrylamide
1.875 ml	Resolving buffer	1.25 ml	Stacking buffer
3.28 ml	Milli-Q H_2O	1 ml	Milli-Q H_2O
Polymerise with:		Polymerise with:	
37.5 µl	10% Ammonium persulphate	17.5 µl	10% Ammonium persulphate
7.5 µl	TEMED	3.5 µl	TEMED

2x SDS-PAGE sample buffer

500 µl	10% SDS
100 µl	2-mercaptoethanol
200 µl	Glycerol
120 µl	Tris-HCl (1M, pH 6.8)
10 µl	1% Bromophenol blue
70 µl	Milli-Q H_2O

Mix 1:1 with sample dilution and boil for 5 minutes.

Coomassie blue

1.25 g Coomassie Brilliant Blue G-250 (BD Biosciences)

225 ml Methanol

45 ml Acetic acid

230 ml Milli-Q H_2O

Filter through Whatman No 1 paper.

10x Electrophoresis buffer

144 g Glycine

30 g Tris

10 g SDS

Bring volume to 1000 ml with deionised water.

Dilute 1:10 with deionised water for use.

Destain solution

100 ml Methanol

100 ml Acetic acid

800 ml Deionised water

Dialysis buffers

Coupling phosphate buffered saline (cPBS)

5.2g $NaH_2PO_4.2H_2O$

23.66g Na_2HPO_4

17.54g NaCl

Bring to final volume to 2000 ml with deionised water.

Adjust pH to range between 7.3 and 7.4 with 0.2 M NaH_2PO_4 or Na_2HPO_4.

Autoclave.

50% glycerol buffer

500 ml 100% glycerol

500 ml cPBS

Autoclave

ELISA

10 x Phosphate buffered saline (PBS)

80g	NaCl
11.35 g	Na_2HPO_4
2 g	KCl
2g	KH_2PO_4

Made up to 1 L with deionised water

Wash Buffer

200 ml	10 x PBS
1 ml	Tween 20

Made up to 2 L with deionised water

Blocking buffer

10 ml	10 x PBS
1 g	Bovine serum albumin (BSA)

Made up to 100 ml with deionised water

Sample diluent

10 ml	10 x PBS
1 g	BSA
0.02 µl	Tween 20

Made up to 100 ml with deionised water

Appendix 2. Supplementary figures

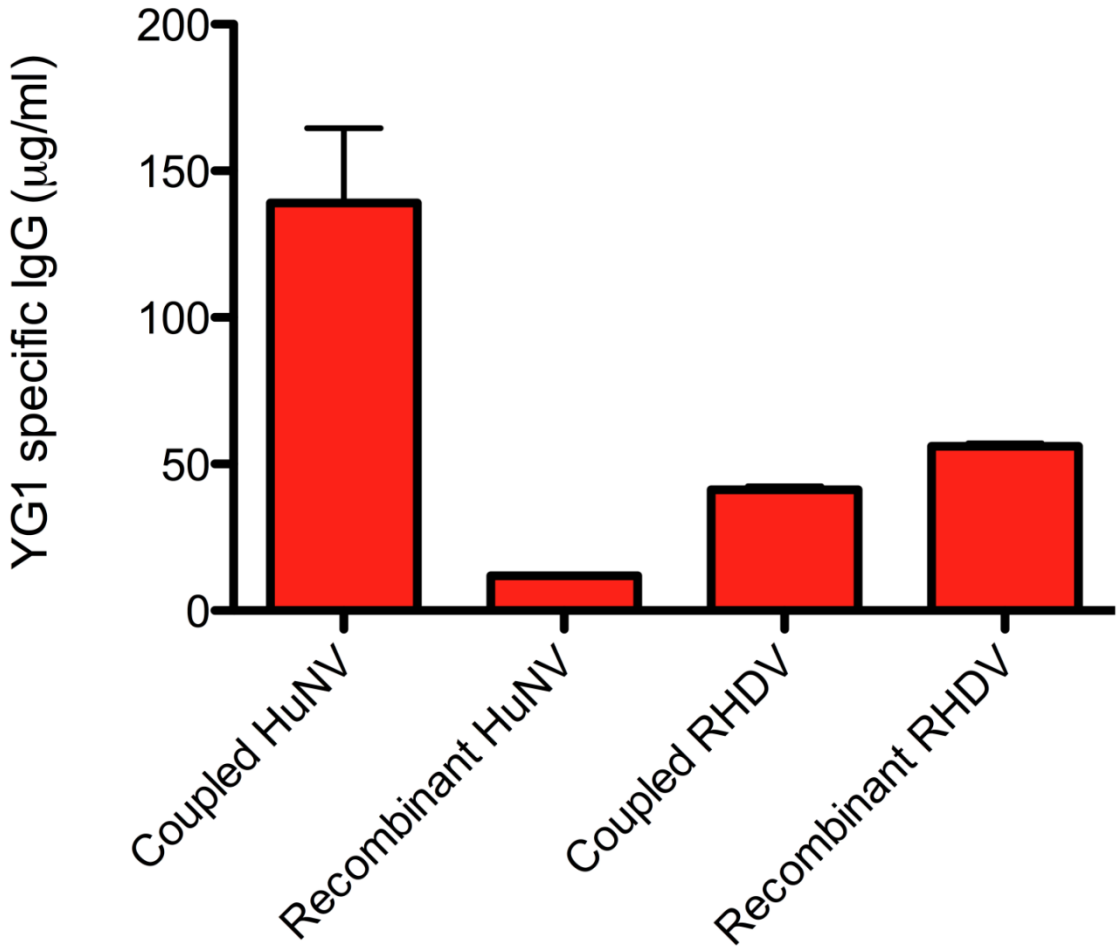

Figure A1. Comparison of serum IgG antibody titres specific for YG1 in rats vaccinated with coupled versus recombinant VLP-YG1

Serum from rats vaccinated with YG1 coupled to VLP was obtained from Sam McClintock and IgG ELISA performed in parallel to my samples. Results showed the coupled form of HuNV-YG1 was 10 times more effective at generating YG1 specific IgG than the recombinant form, while the two forms of RHDV showed no significant difference.